An improved evaluation of ^{17}O system (preliminary)

IAEA
International Atomic Energy Agency

Zhenpeng Chen[1], Libo Zhou[2], Yeying Sun[1], Tao Ye[3]

1 Physics Department, Tsinghua University, Beijing, China

2 Graduate School, China Academy of Engineering Physics, Beijing, China

3 Institute of Applied Physics and Computational Mathematics, Beijing, China

IAEA Meeting, 20-23, June, 2022

contents

0 Introduction

An improved evaluation of ^{17}O system has been done. Compared with the 2021 report, the improvements mainly include these 4 aspects:

(1). In the low energy region (6.2 MeV), the white source measurements of KFK were carefully smoothen to take into account more neutron elastic scattering differential cross sections. It can compensate for the absence of experimental neutron total cross sections in the 0.9 to 1.8 MeV energy region.

(2). Some reaction channels in the high energy region are no longer expressed by the parameter 'total width of reduced channels'--Γ, but expressed by 'polynomials + peak' in the background and also included in the process of fitting data. In this way, all available experimental data are used in the fitting process, and the integral cross sections of all reaction channels are given.

Introduction

(3). The 'total width of reduced channel'--Γ, represents only the high energy contribution of inelastic scattering, as well as the high energy contribution of ejected alpha particles, and other residual reactions that are not considered. In the process of fitting, a careful distinction of them is made.

(4). Trying to make an evaluation file with ENDF-6 Formats. This file requires at least 1000 neutron incident energy points. One difficulty is that the error propagation theory can be used to calculate all types of covariance matrix, but the matrix volume is too large and the file is too long. we don't know which ones have practical value and which ones don't.

contents

1 The reaction channels

For n+^{16}O, include 9 channels in R-matrix formula:

‘ ^{16}O(n,n_0)^{16}O$_0$ ’ ‘ ^{16}O(n,n_1)^{16}O$_1$ ’ ‘ ^{16}O(n,n_2)^{16}O$_2$ ’
‘ ^{16}O(n,n_3)^{16}O$_3$ ’ ‘ ^{16}O(n,n_4)^{16}O$_4$ ’

‘ ^{16}O(n,α_0)^{13}C$_0$ ’ ‘ ^{16}O(n,α_1)^{13}C$_1$ ’ ‘ ^{16}O(n,α_2)^{13}C$_2$ ’
‘ ^{16}O(n,α_3)^{13}C$_3$ ’

And these channels in formula ‘polynomial + peaks’:

‘ ^{16}O(n,p)^{16}N ’ ‘ ^{16}O(n,d)^{15}N ’ ‘ ^{16}O(n,t)^{14}N ’
‘ ^{16}O(n,2n)^{15}O ’ ‘ ^{16}O(n,np)^{15}N ’ ‘ ^{16}O(n,nα)^{12}C ’

1 The reaction channels

For $\alpha+^{13}C$, include 9 *reverse* channels in R-matrix formula:

‘ $^{13}C(\alpha,\alpha_0)^{13}C_0$ ’ ‘ $^{13}C(\alpha,\alpha_1)^{13}C_1$ ’ ‘ $^{13}C(\alpha,\alpha_2)^{13}C_2$ ’
‘ $^{13}C(\alpha,\alpha_3)^{13}C_3$ ’

‘ $^{13}C(\alpha,n_0)^{16}O_0$ ’ ‘ $^{13}C(\alpha,n_1)^{16}O_1$ ’ ‘ $^{13}C(\alpha,n_2)^{16}O_2$ ’
‘ $^{13}C(\alpha,n_3)^{16}O_3$ ’ ‘ $^{13}C(\alpha,n_4)^{16}O_4$ ’

1 The reaction channels

A *reduced* channel total width (used for 8 to 30 MeV), which represents the total contribution of other residual channels. For example,

1. inelastic scattering : $^{16}O(n,n_k)^{16}O_k$, k = 5,6,7,8,…;

2. (n,α) : $^{16}O(n,\alpha_k)^{13}C_k$, k = 4,5,6,…, which emits only one α;

3. other residual channels:

‘ $^{16}O(n,2np)^{14}N$ ’ ‘ $^{16}O(n, n2p)^{14}C$ ’ ‘ $^{16}O(n, np\alpha)^{10}B$ ’

contents

2 The relationship of cross sections

(n, tot) = (n, el) + (n, inl) + (n, α)
+ (n, p) + (n, d) + (n, t)
+ (n, 2n) + (n, np) + (n, nd) + (n, nα)
+ (n, g)
+ (n, Redu-all),

which can be used to describe the experimental data of (n, tot).

(n, el) = (n, el),

which can be used to describe the experimental data of neutron *elastic* scattering;

2 The relationship of cross sections

(n, inl) = **(n,n_1) + (n,n_2) + (n,n_3) + (n,n_4) + (n, Redu-inl)**, which can be used to describe the experimental data of neutron total *inelastic* scattering. In EXFOR, only has this kind of data.

(n, Redu-inl) represents *inelastic* scattering part in **(n, Redu-all);**

2 The relationship of cross sections

- **(n, α) = (n,α_0) + (n,α_1) + (n,α_2) + (n,α_3) + (n, Redu-α)**, which can be used to describe the experimental data of total (n,α). In EXFOR, only has this kind of data.
- **(n, Redu-α)** represents (n,α) part in **(n, Redu-all).**

- **(n, p), (n, d), (n, t), (n, 2n), (n, np), (n, nd), (n, nα),** Which were determined by fitting experimental data.
- **(n, g)**, which is taken from ENDF/B-VIII, put into the background of **(n, tot).**

2 The relationship of cross sections

- **(n, Redu-all) = (n, Redu-inl) + (n, Redu-α) + (n,Redu-rest),** this formula explains that the total contribution of the reduced channel can be divided into three parts on the right.
- **(n, redu-all)** is determined by fitting all data,
- **(n, redu-inl)** is determined by fitting total non-elastic scattering data,
- **(n, Redu-α)** is determined by fitting total (n,α) data.
- **(n, Redu-rest)** is determined in the process of fitting all data.
- **(α, n) = (α, n_0) + (α, n_1) + (α, n_2) + (α, n_3) + (α, Redu)**, which can be used to describe the experimental data of total **(α, n)**. In EXFOR, only has this kind of data.

contents

3 White source measurements of KFK

In the low energy region (0.5 to 6.2 MeV), the white source measurements of KFK were carefully smoothen to take into account more neutron elastic scattering differential cross sections. It can compensate for the absence of experimental neutron total cross sections in the 0.8 to 1.8 MeV energy region.

The data of (I.Schouky, S.Cierjacks, EXFOR-20955000) includes 2114 energy points and 10 angles, with uncertainty in flux (3%), give a total error of 7 to 10%.

3 White source measurements of KFK

For the region below 0.9 MeV, there is a lot of oscillation, so direct smoothing is adopted, and peaks and valleys are ignored. The specific operation is to use multiple **Savitzky-Golay** filtering fitting method to smooth the data with large oscillation quickly, and then use binomial smoothing method to smooth the small fluctuation.

Formant peaks are visible above 0.9 MeV. To preserve these formants, the energy region can be segmented by the resonant energy level. For the part between two peaks, **binomial smoothing** method is mainly used, because this method can ensure that the values of the two endpoints before and after smoothing remain unchanged, that is, the height of the peak remains unchanged.

3 White source measurements of KFK

Another advantage of binomial smoothing is that the part near the peak is better preserved in its original form, that is, the width of the peak does not change much.

In addition, for the part between two peaks, Savitzky-Golay filtering fitting method and local weighted regression method are also used (Essentially it is also an adjacency averaging method, where the closer to the center point the greater the weight). Because these two methods change the values at the endpoints, additional correction for peaks is required.

3 White source measurements of KFK

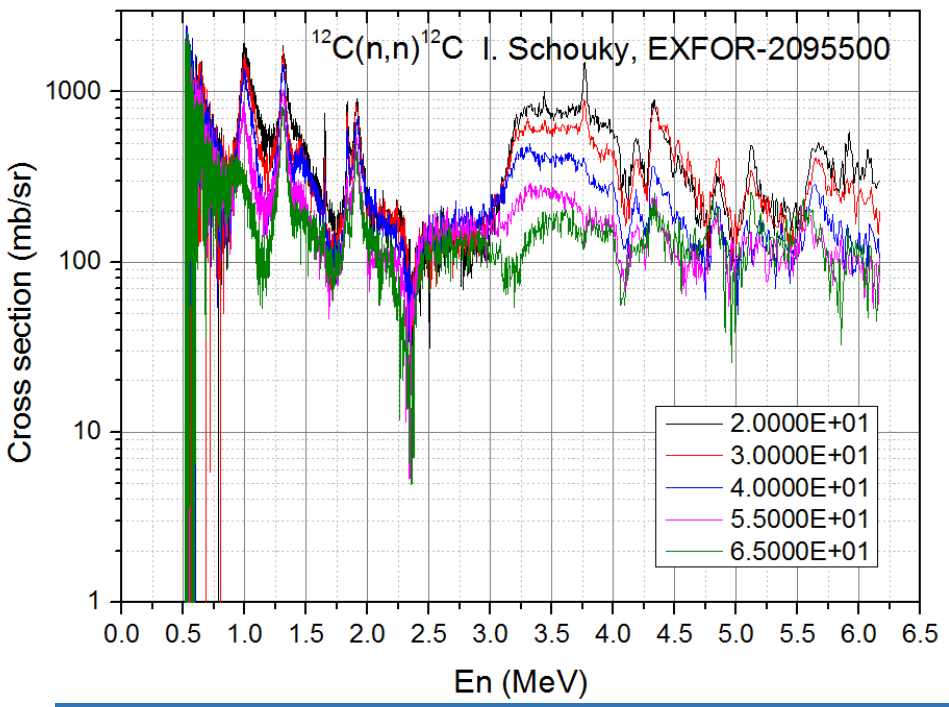

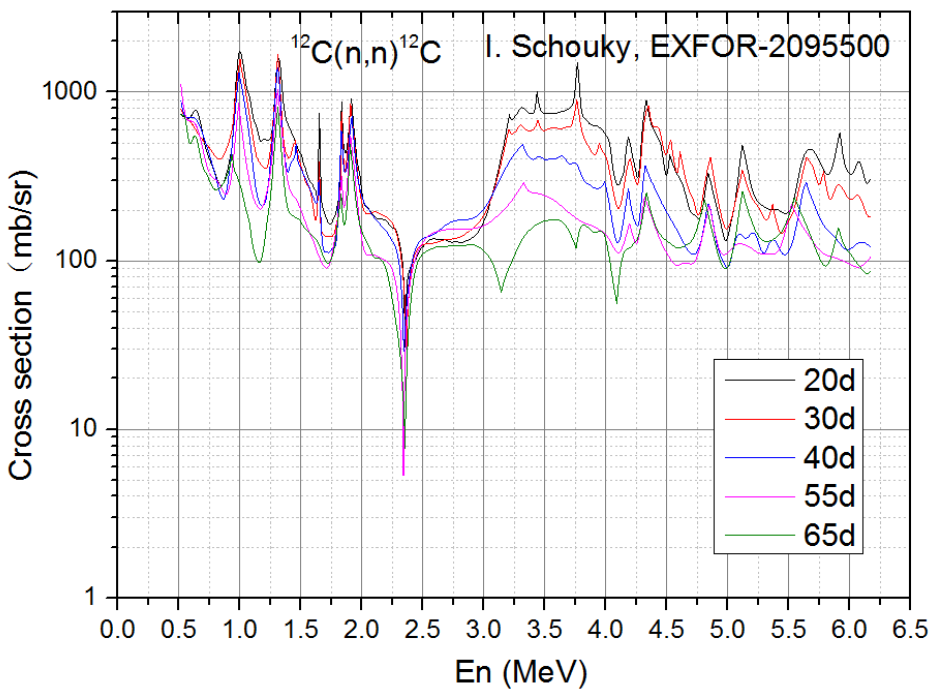

Fig.1. Comparison of data before and after smoothing at 20,30,40,55 and 65 degrees

3 White source measurements of KFK

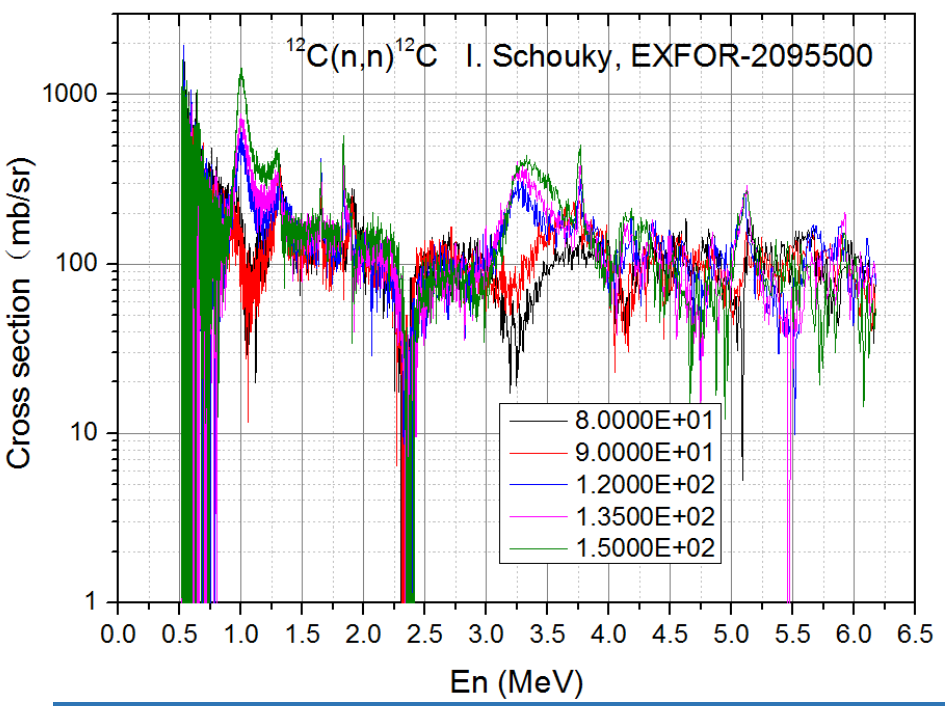

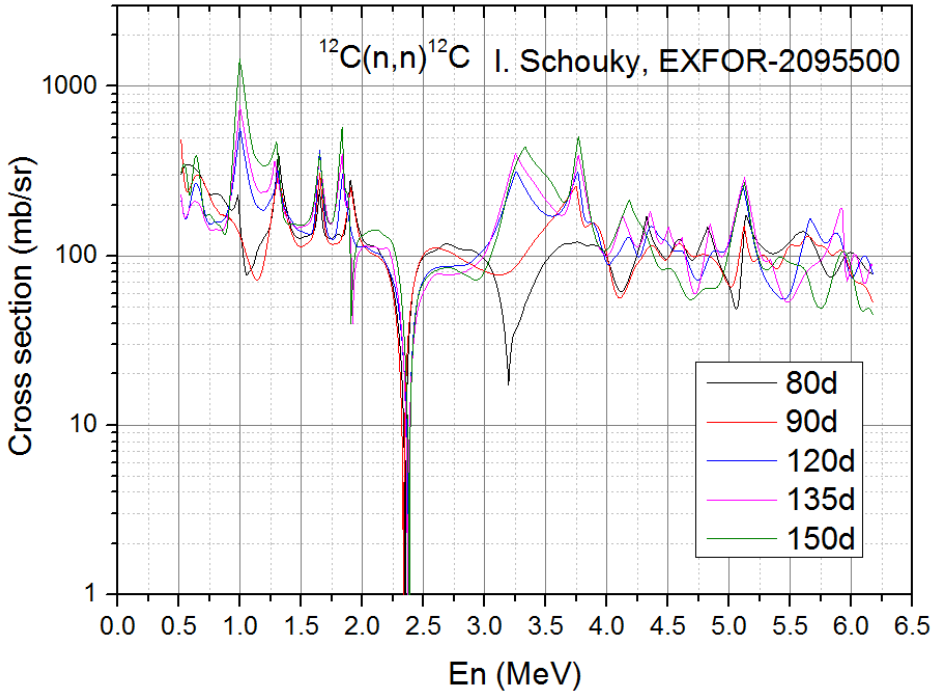

Fig.2. Comparison of data before and after smoothing at 80,90,120,135 and 150 degrees

From 0.8 to 1.8 MeV, the smoothed excitation function was used to extract 10 angular distributions, which played a good constraint role in data fitting. Refer to Appendix I.

contents

4 Current situation of data fitting

All the levels of ^{17}O listed in 'Table(1993TI07): Energy levels of ^{17}O' have been used. A total of 186 energy levels were used, and the parameters of all energy levels were determined by fitting experimental data.

The energy range of experimental data is 1e-7 to 32 MeV. The current fitting for experimental data looks good. Refer to figures as follow pages:

4 Current situation of data fitting

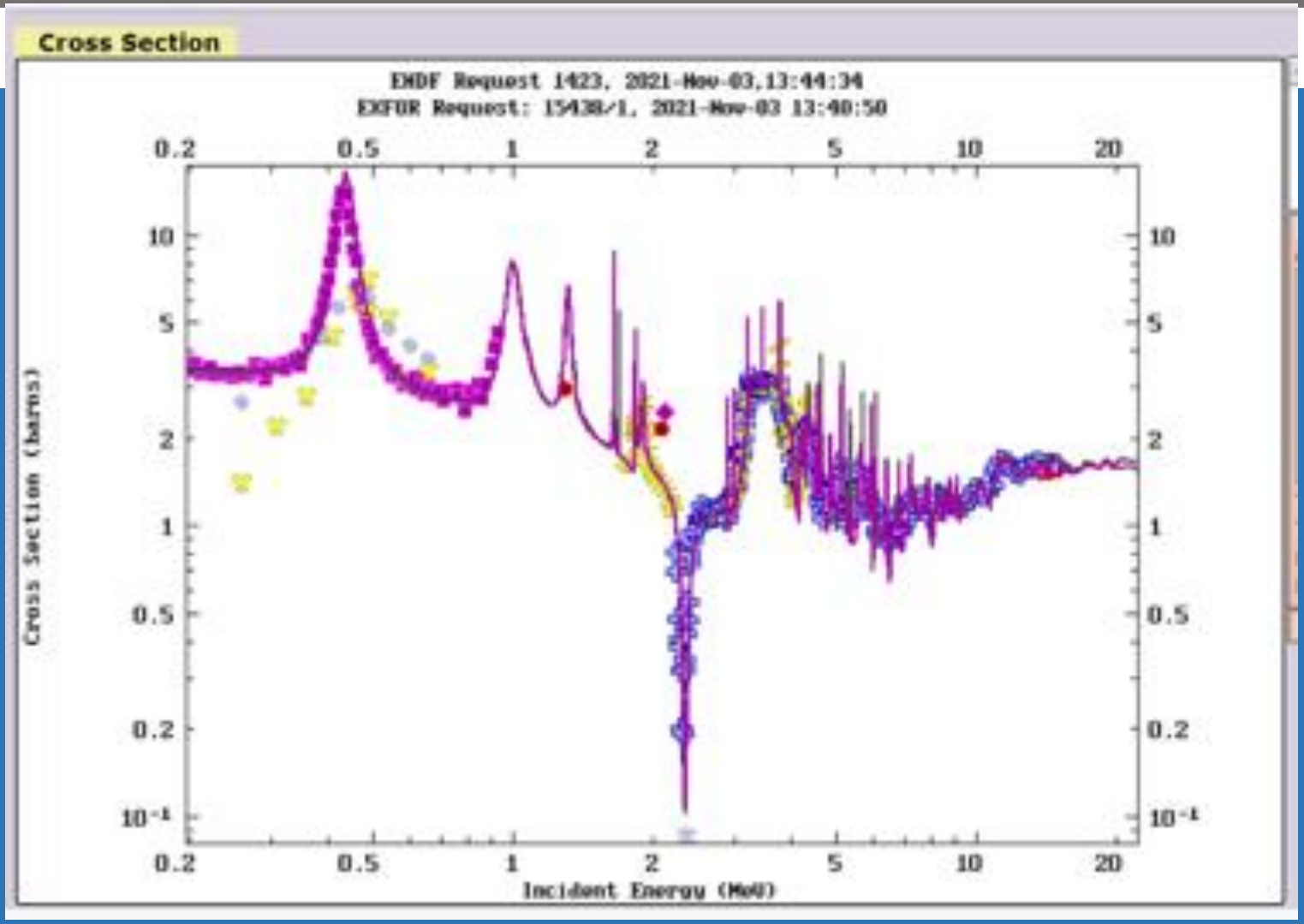

Figure3. The (n,tot) cross section, grey line represents ENDF/B-VIII.0, purple line represents RAC2022. Below 20 MeV, they are very close. Above 20 MeV, there is a little difference, but this area lacks experimental data constraints.

In this comprehensive fitting, the data of (n, tot) plays a dominant function.

4 Current situation of data fitting

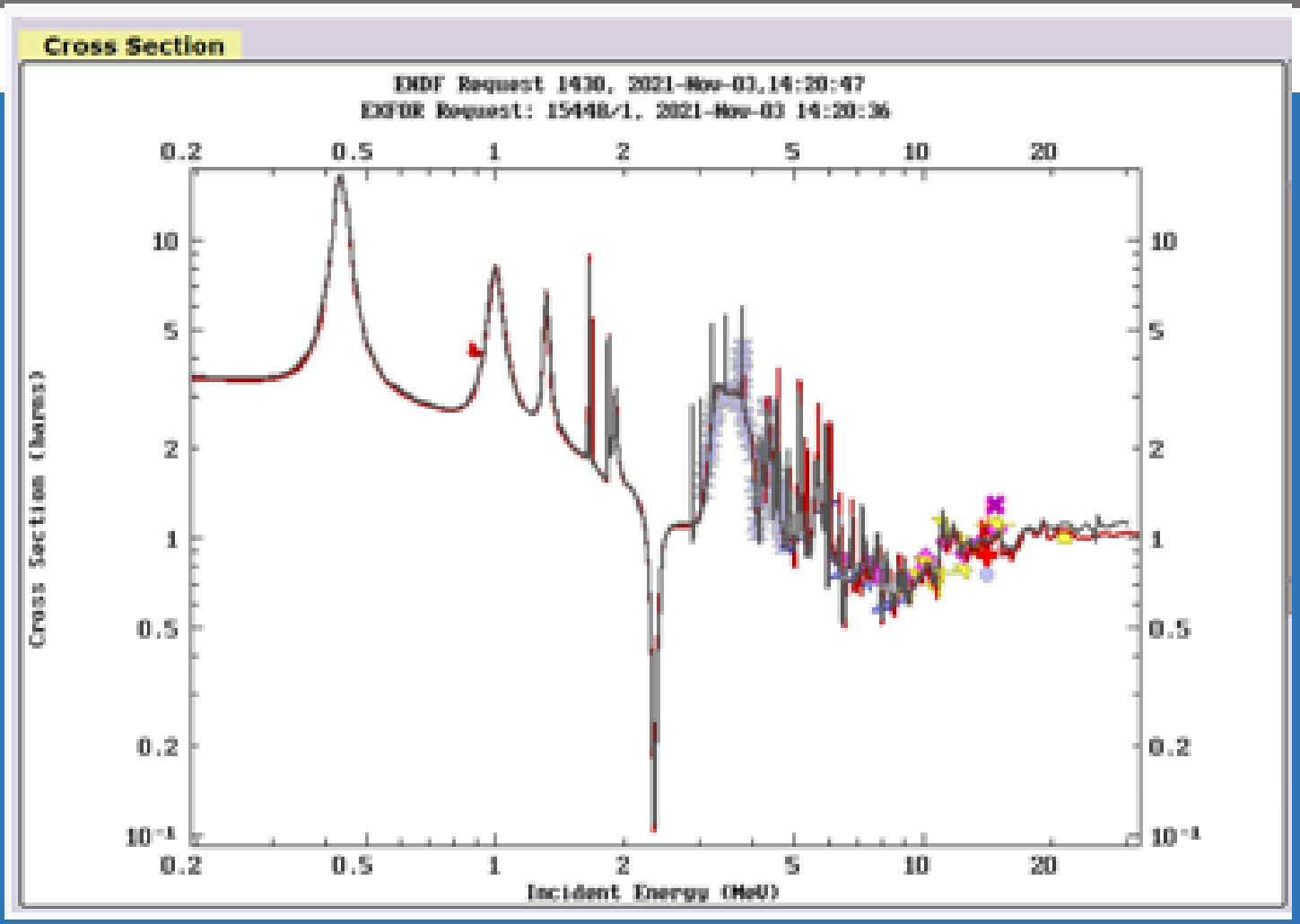

Figure4. The (n,el) scattering cross section, brown line represents ENDF/B-VIII.0, grey line represents RAC2022. Below 20 MeV, they are very close, In this region, the elastic scattering differential cross section plays the decisive role, and the data fitting situation is shown in Appendix I. Above 20 MeV, there is a little difference, but this area lacks experimental data constraints.

4 Current situation of data fitting

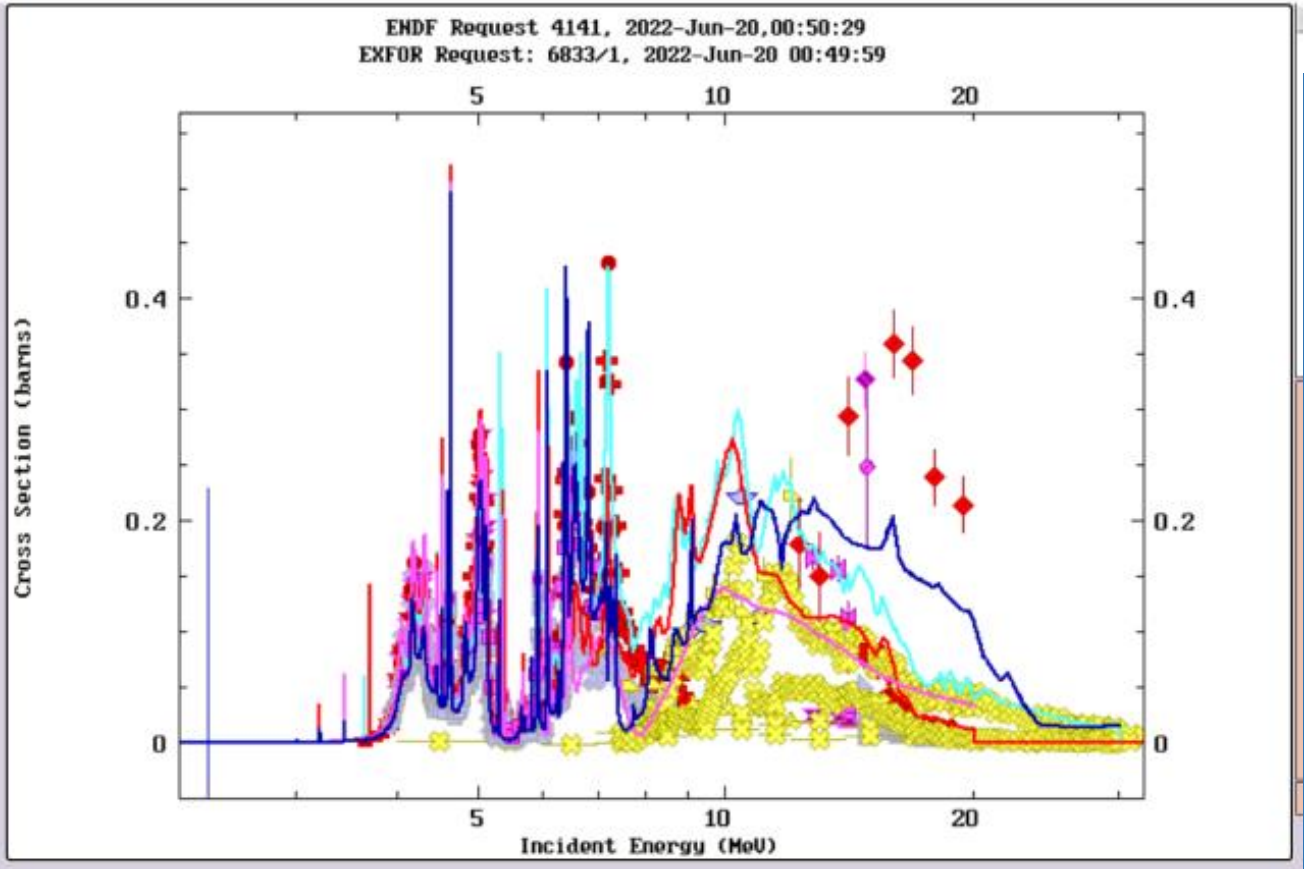

The (n,α) cross section, blue line represents ENDF/B VIII.0, dark blue line represents RAC2022. Below 7 MeV, they are close. In the 7 to 12 MeV range, there is a significant difference, but RAC2022 is closer to the experimental data. Above the 12 MeV range, RAC2022 is significantly greater than ENDF/B VIII.0, and the experimental data of (n, α) have large differences. It should be emphasized here that in this kind of comprehensive evaluation, the fitting value of (n,α) depends on all experimental data instead of (n,α) data merely.

4 Current situation of data fitting

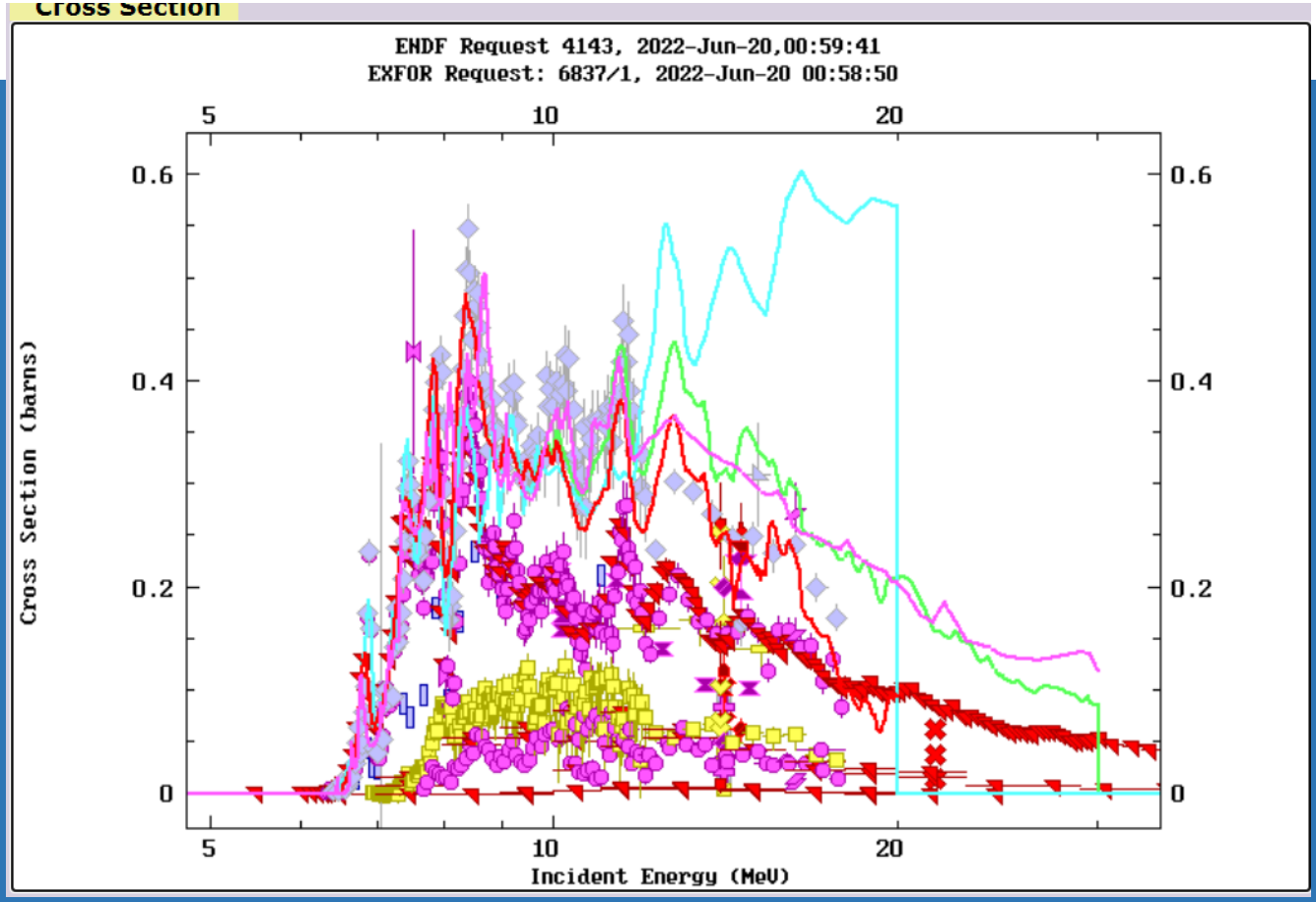

The (n,inl) cross section, green line represents ENDF/B VIII.0, pink line represents RAC2022. Below 12 MeV, they are close. Between 12 and 16 MeV, there is a significant difference, but RAC2022 is closer to the latest experimental data (grey points), that is Boromiza (2020) on (n, inl), which play a positive role of constraint and obvious improvement. It may have a positive effect on (n,α) and (α,n) evaluation improvement. Above 16 MeV ENDF/B VIII.0 and RAC2022 are closed.

4 Current situation of data fitting

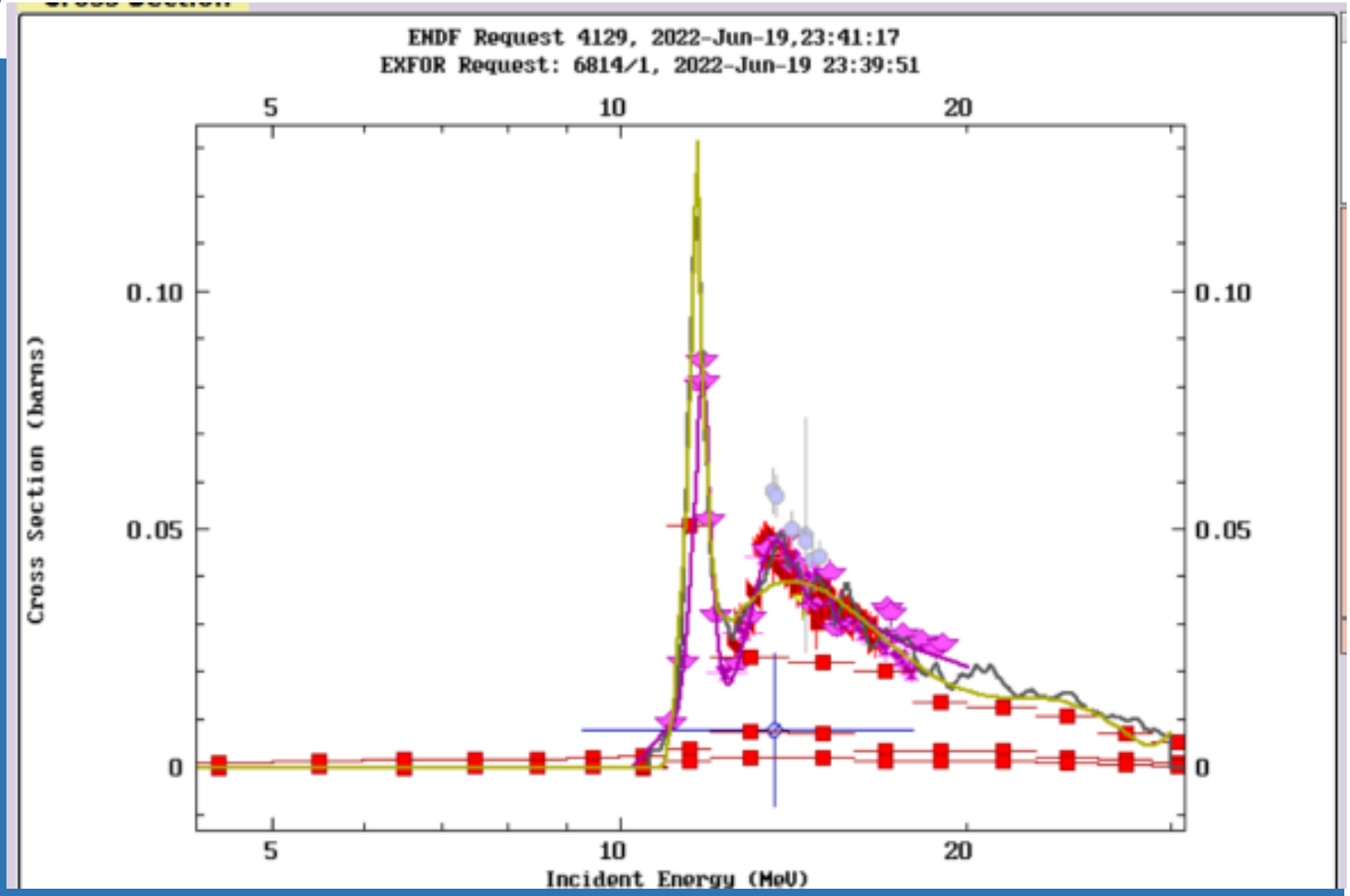

(n,p), The yellow line represents RAC, the black line represents ENDF/B-VIII.0, and the pink line represents CENDL

4 Current situation of data fitting

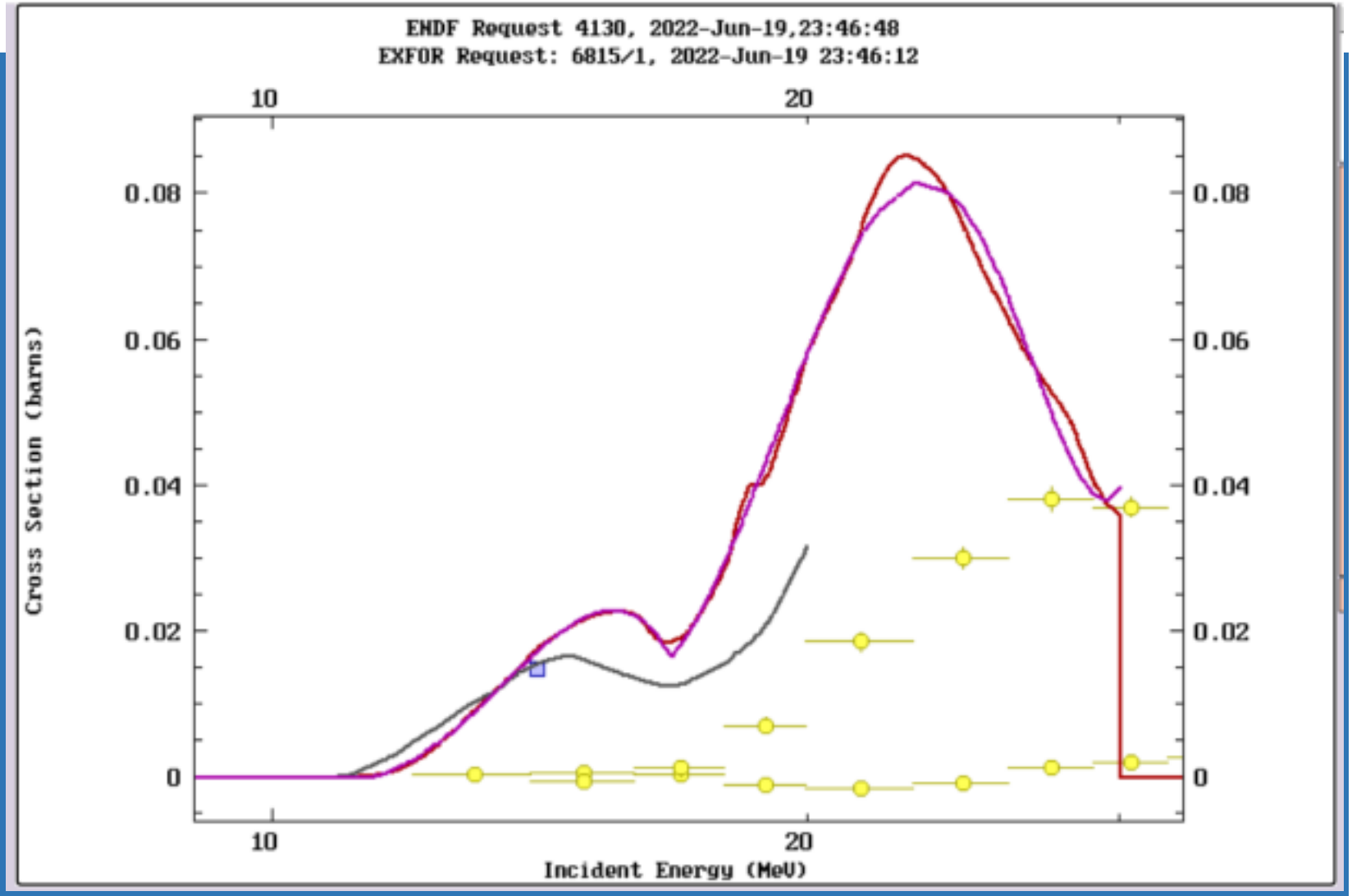

(n,d), The pink line represents RAC, the brown line represents ENDF/B VIII.0, they are closed. And the black line represents CENDL

4 Current situation of data fitting

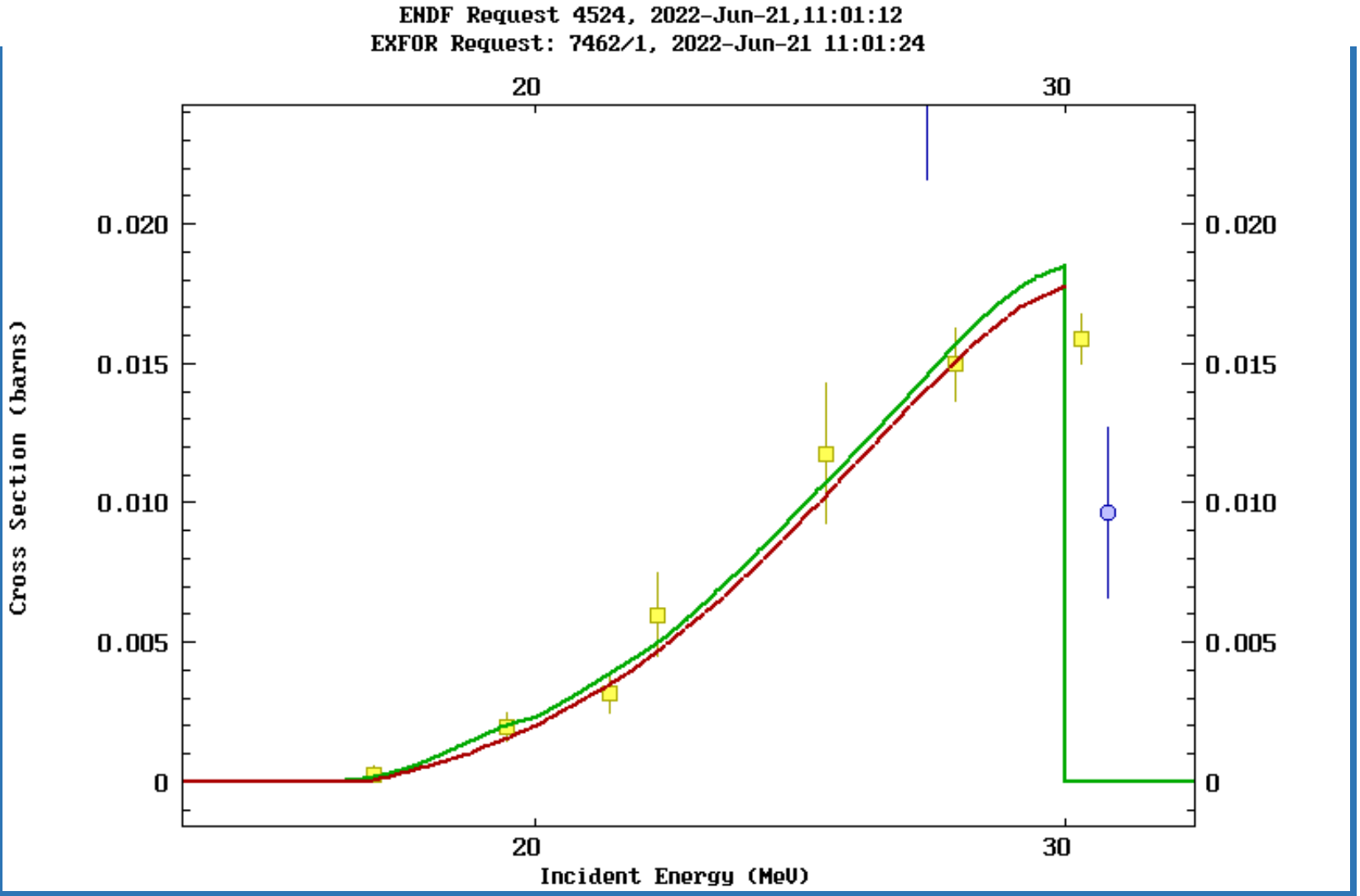

(n,2n), The brown line represents RAC, the green line represents ENDF/B-VIII.0 , they are closed.

4 Current situation of data fitting

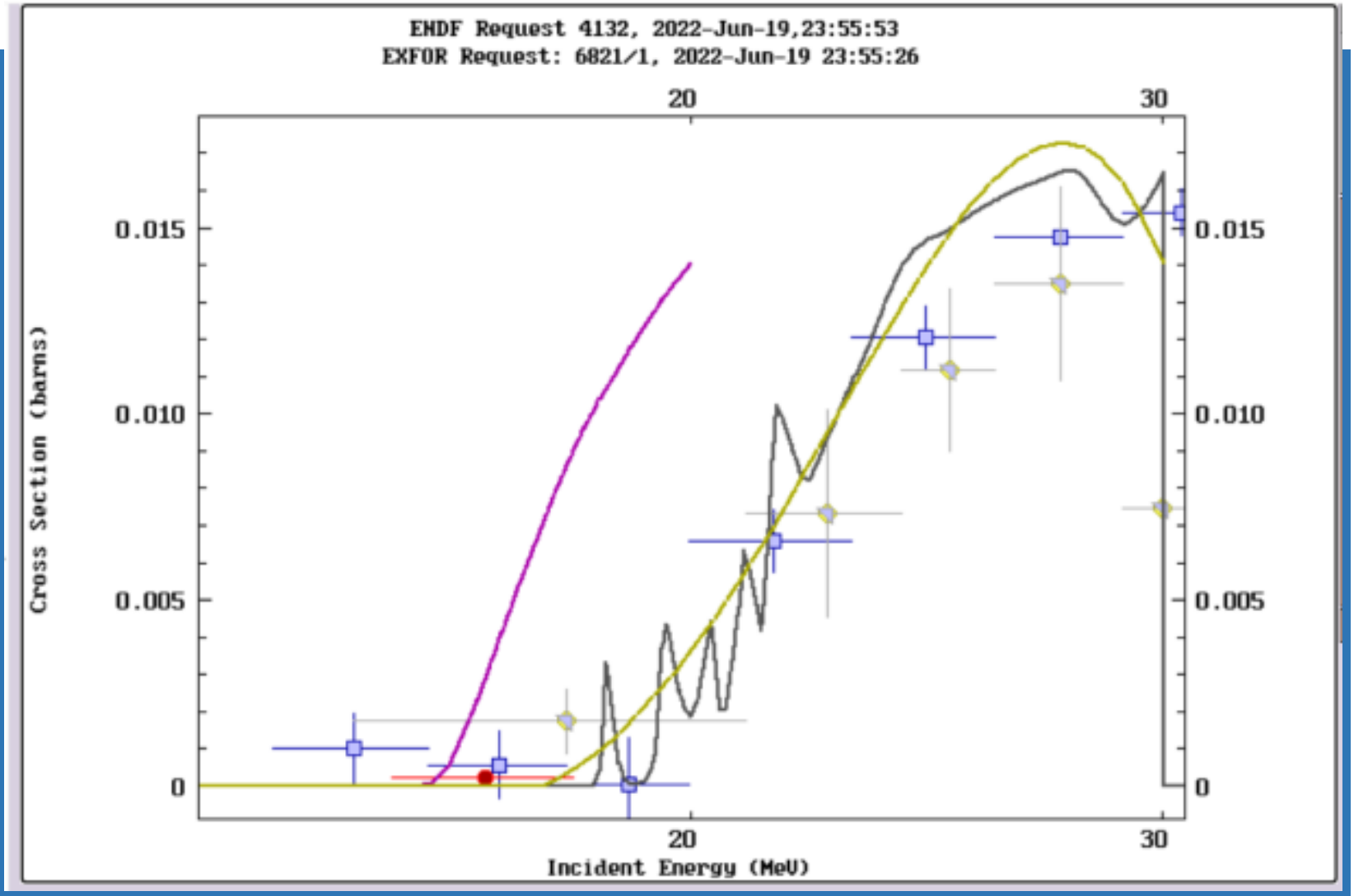

(n,t), The green line represents RAC, the black line represents ENDF/B VIII.0, and the purple line represents CENDL.

4 Current situation of data fitting

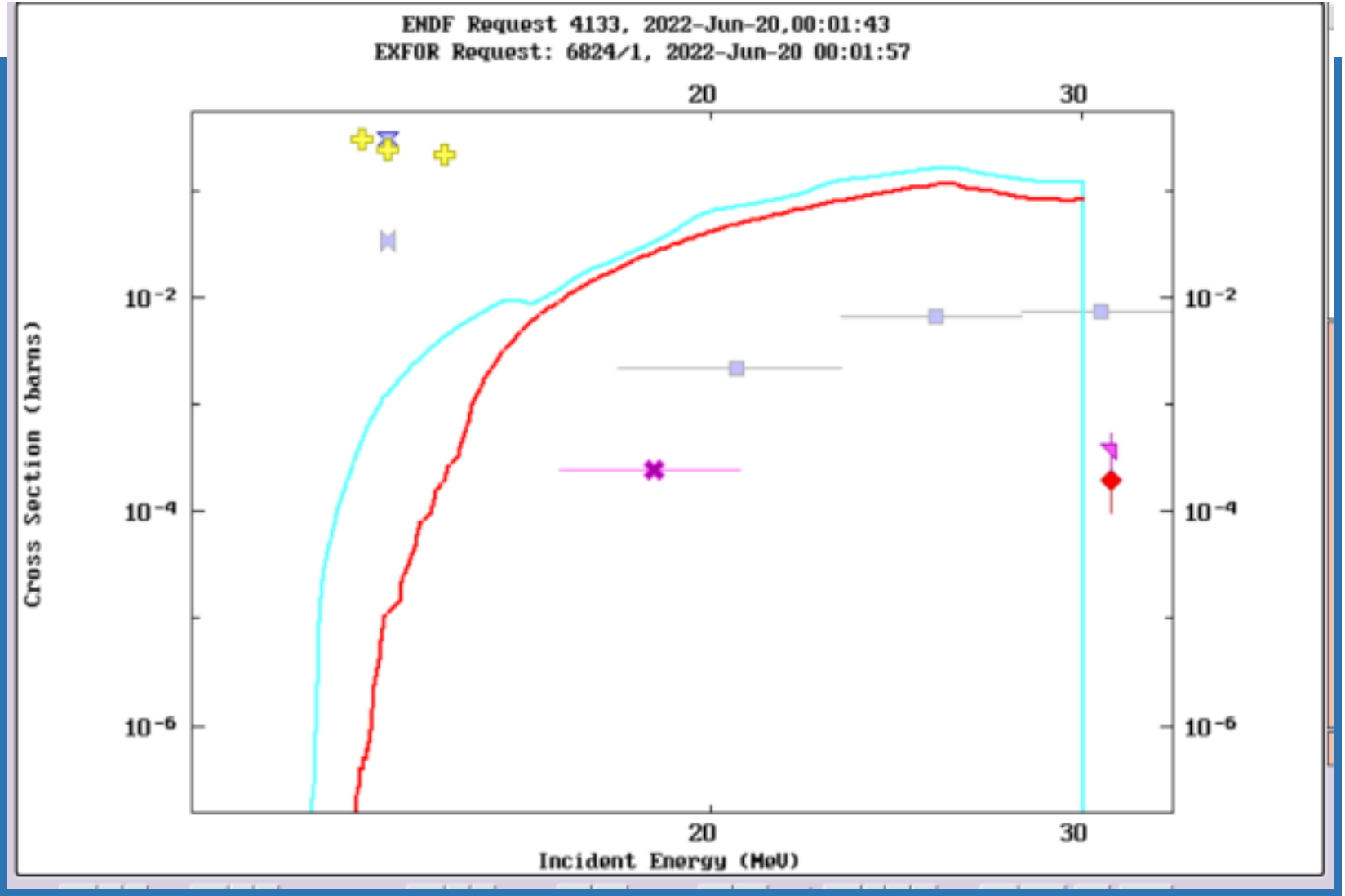

(n,np), The red line represents RAC, the blue line represents ENDF/B VIII.0.

4 Current situation of data fitting

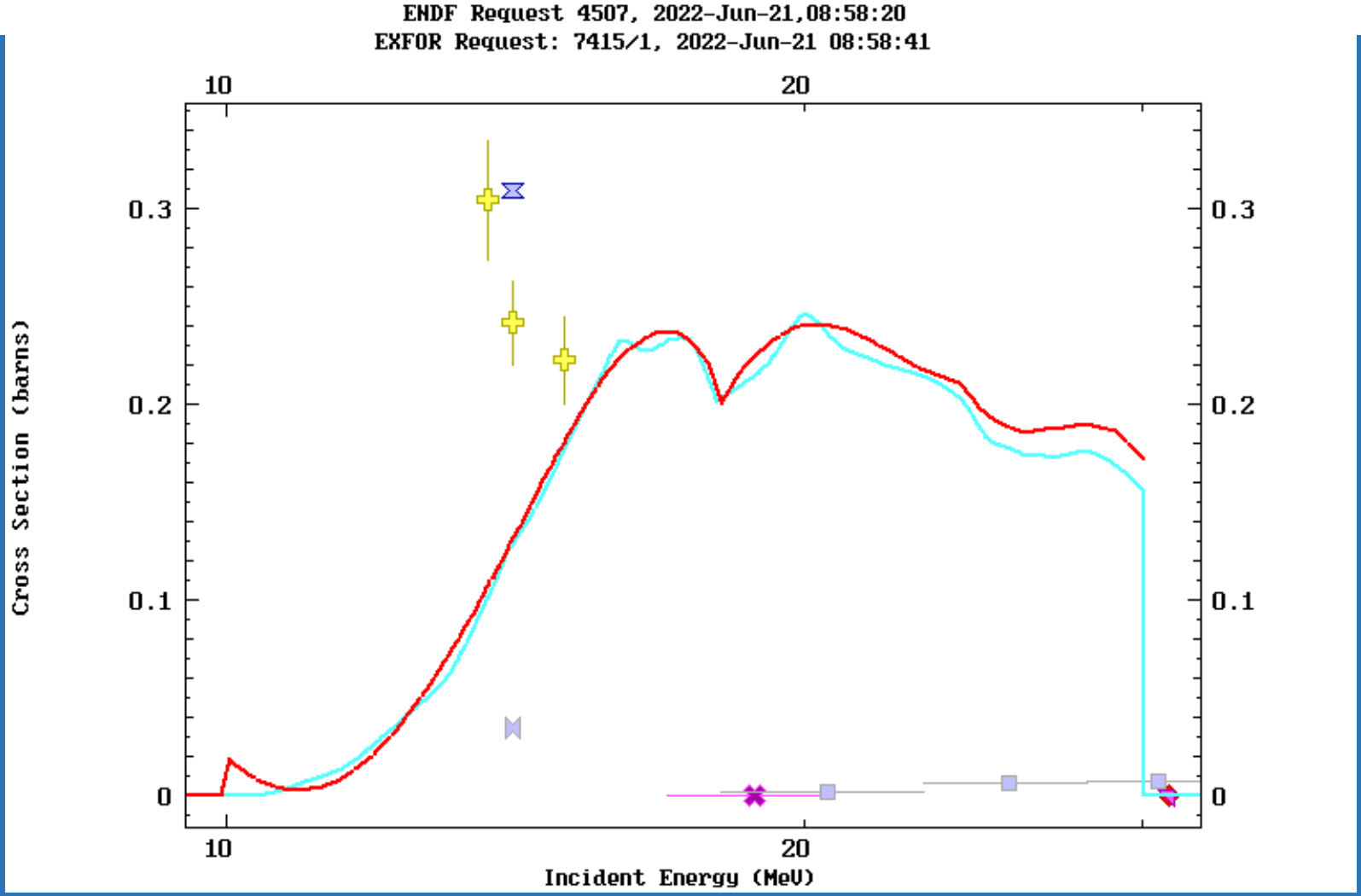

(n,na), The red line represents RAC, the blue line represents ENDF/B VIII.0.

4 Current situation of data fitting

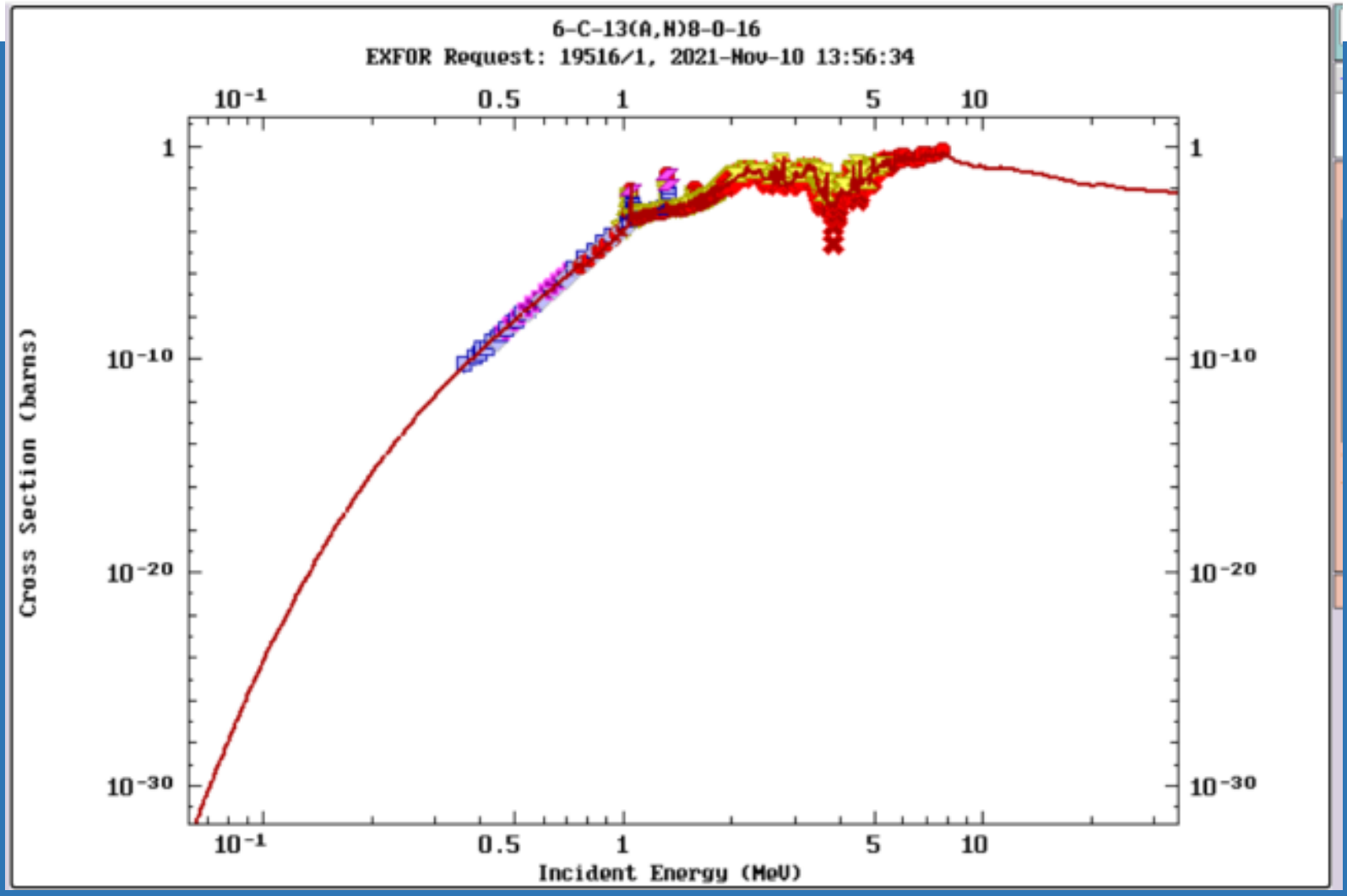

The (α,n) cross section, no evaluation value can be found in ENDF files, red line represents RAC2022. Below 8 MeV, RAC2022 is very close to the experimental value. Above 8 MeV, the (α, n) evaluation depends on other data, especially (n,α) cross section.

4 Current situation of data fitting

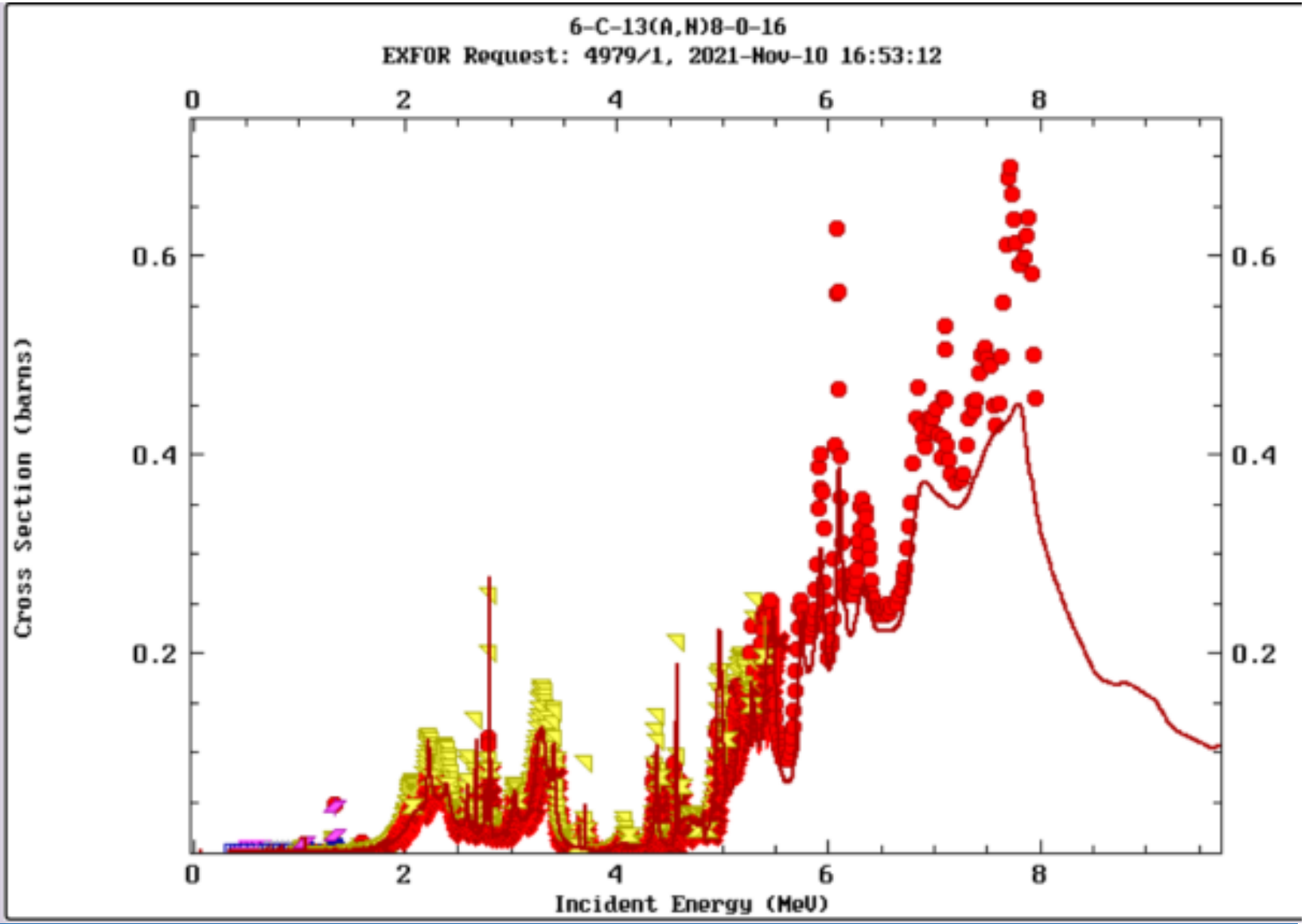

The (α,n) cross section

contents

5 Integral cross section calculation values

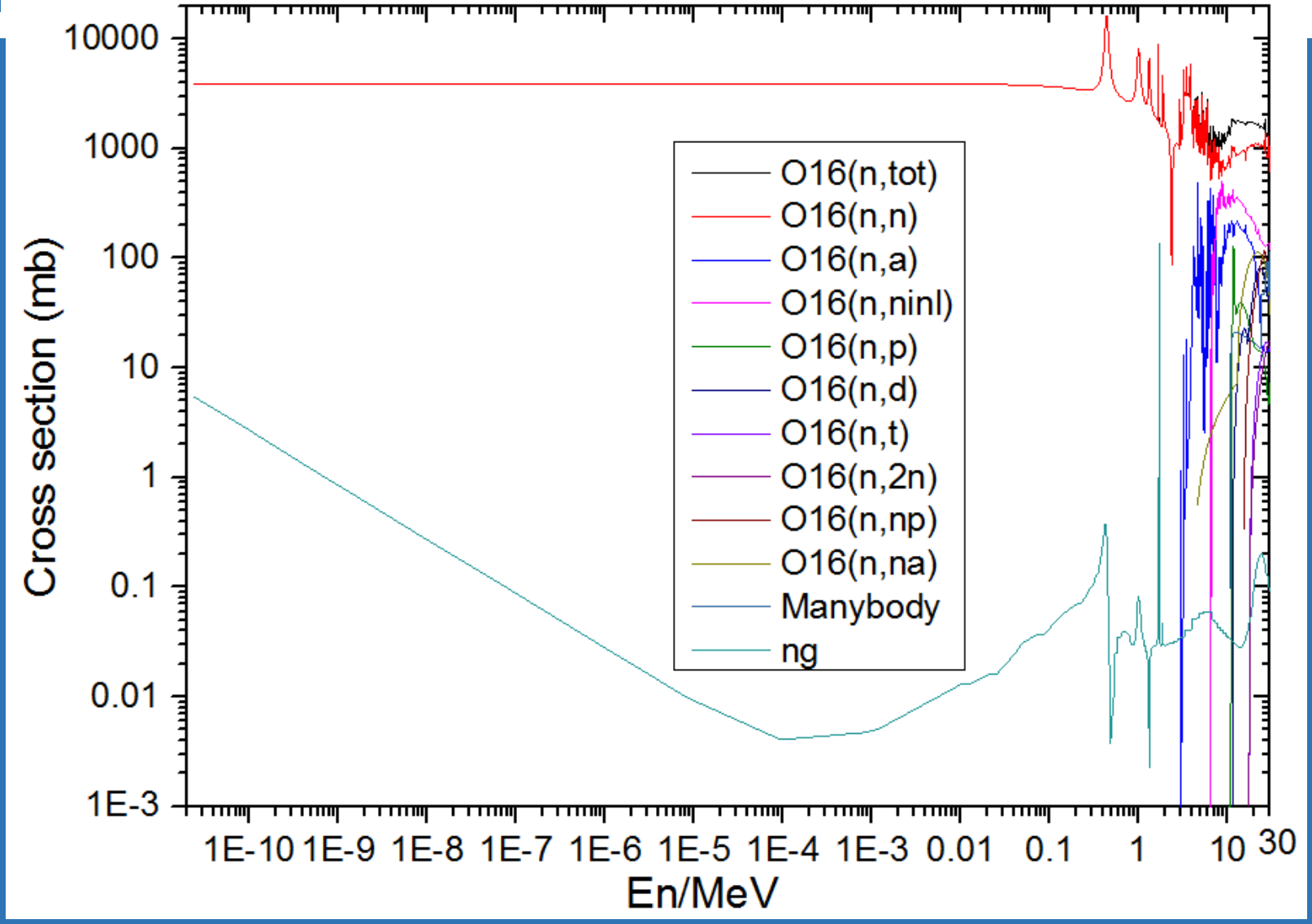

The calculated integral cross section from 1e-11 to 30 MeV of RAC-2022.

5 Integral cross section calculation values

The relation of calculated integral cross section:

(n, tot) = (n, el) + (n, inl) + (n, α) + (n, rest)

(n, inl) = (n, n1) + (n, n2) + (n, n3) + (n, n4) + (n, Redu-inl)

$(n, \alpha) = (n, \alpha_0) + (n, \alpha_1) + (n, \alpha_2) + (n, \alpha_3) + (n, \text{Redu-}\alpha)$

(n, rest) = (n,p) + (n,d) + (n,t) + (n,2n) + (n,np) + (n,na) + (n,g) + (n, Redu-rest)

5 Integral cross section calculation values

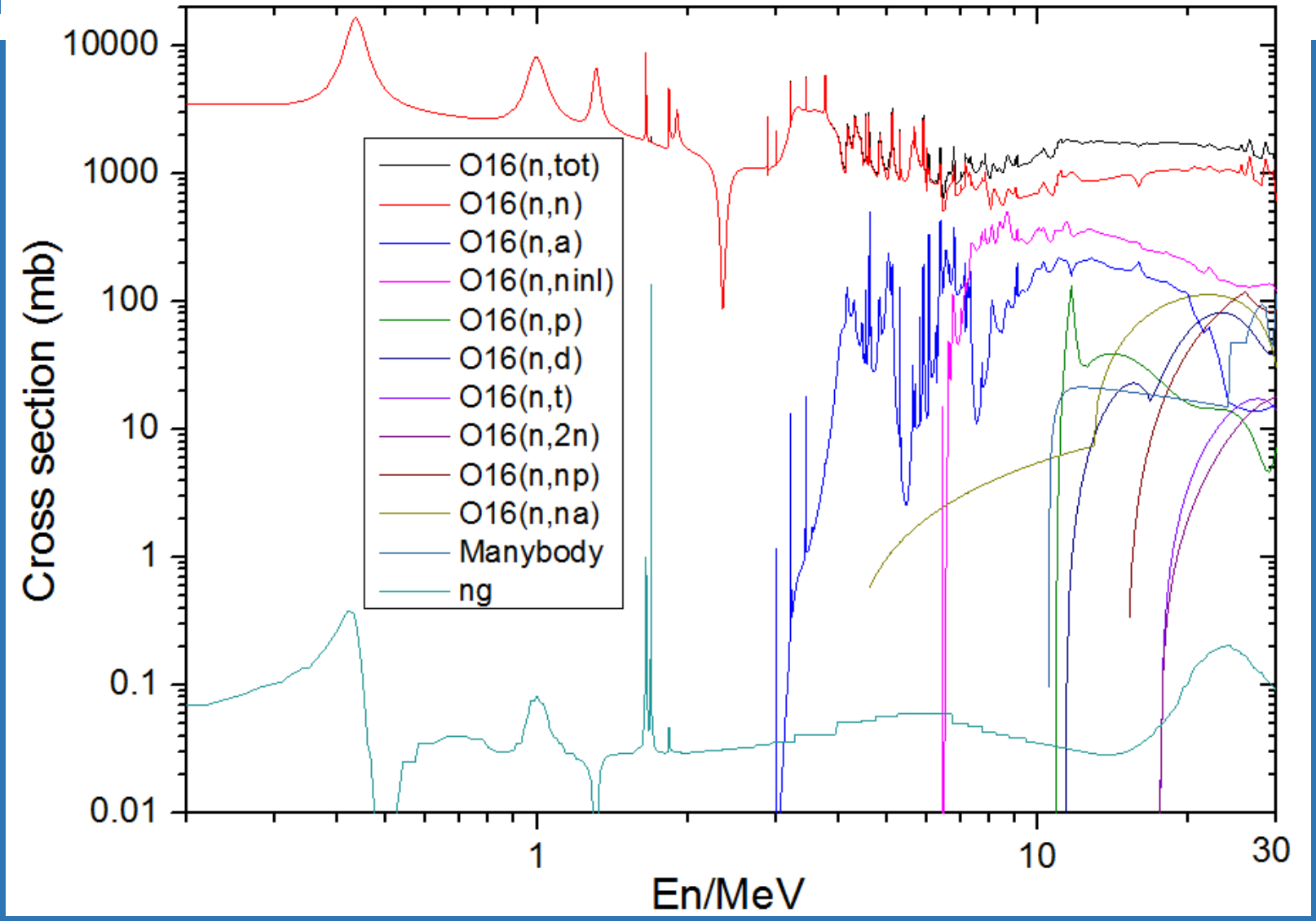

The reaction channel with determined calculated values

5 Integral cross section calculation values

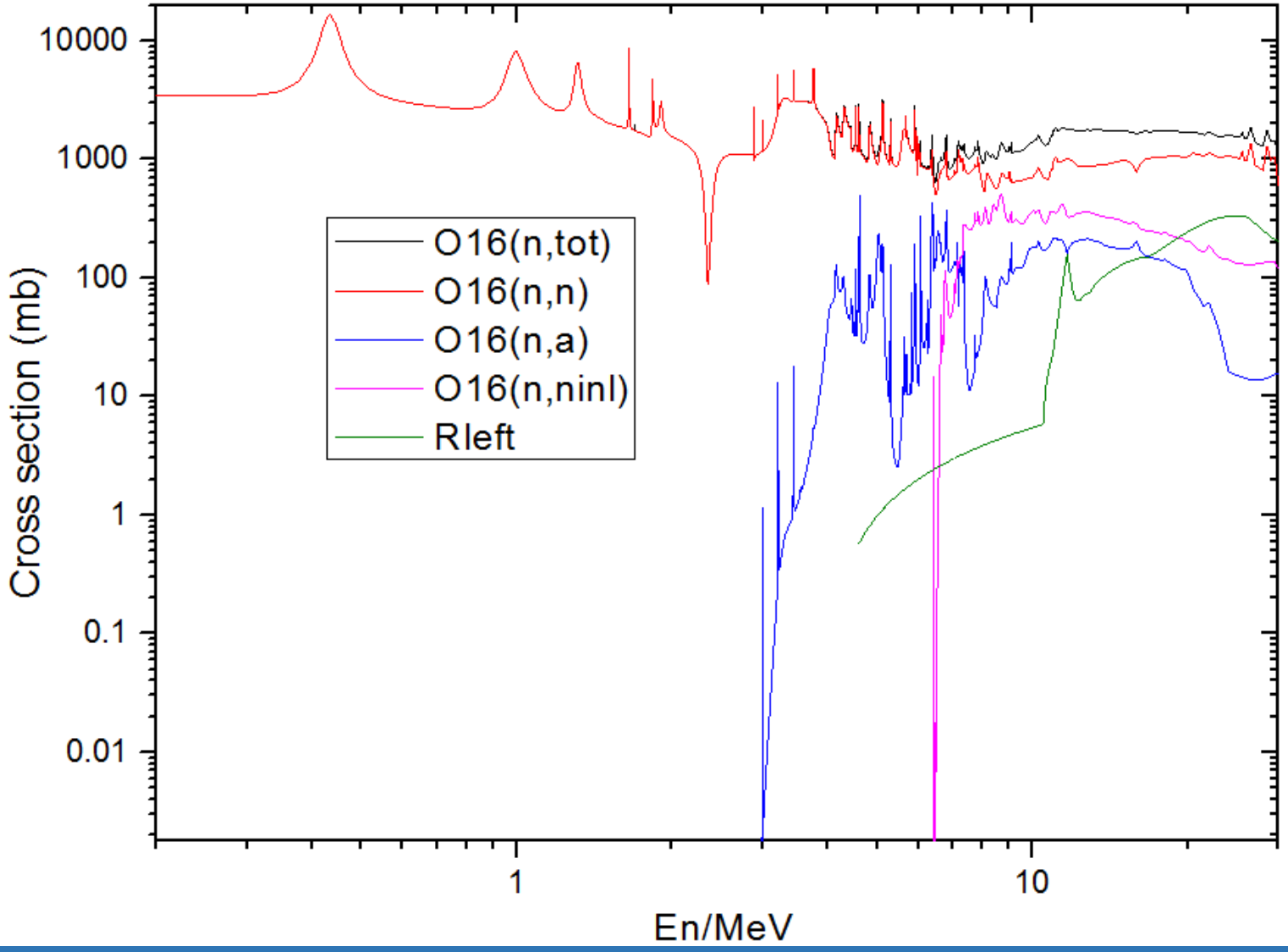

The reaction channel with the maximum calculated value, except for (n, el), (n, inl) and (n,a), the contribution of 'residual reaction' is relatively small.

5 Integral cross section calculation values

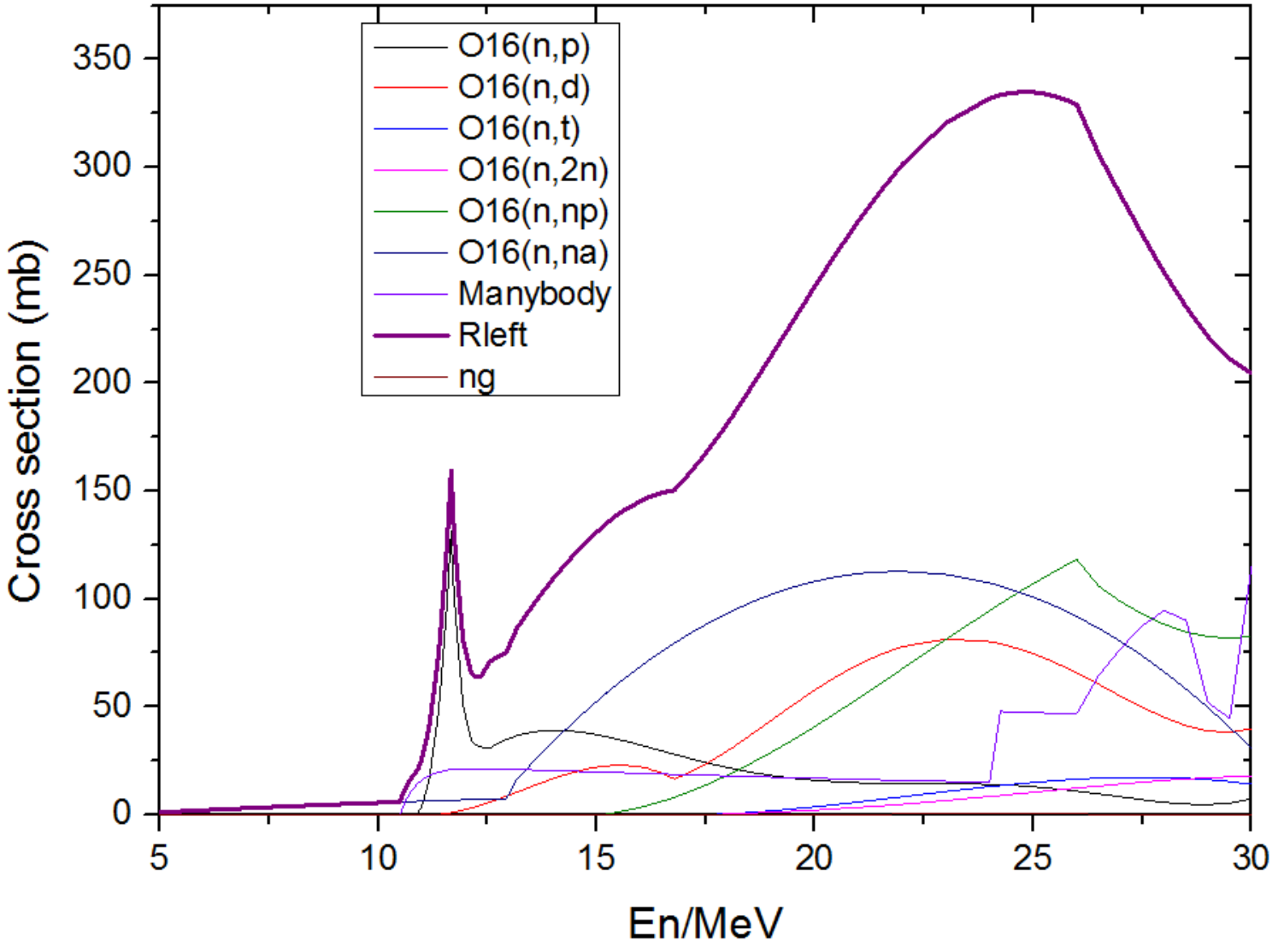

The contributions of the various reaction channel in the 'residual reactions'.

5 Integral cross section calculation values

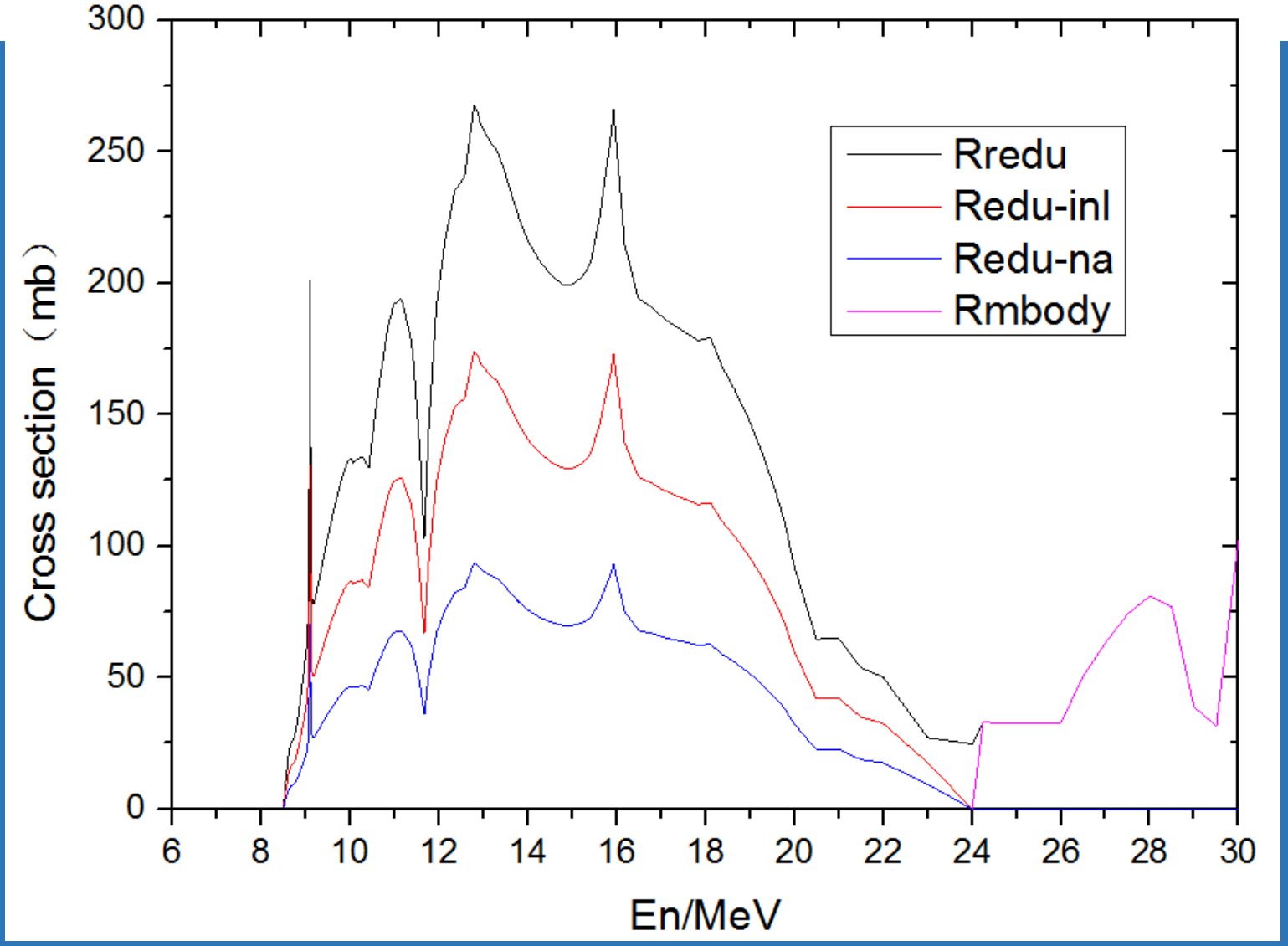

The contributions of the various reaction channel in the ‘total reduced channel’.

5 Integral cross section calculation values

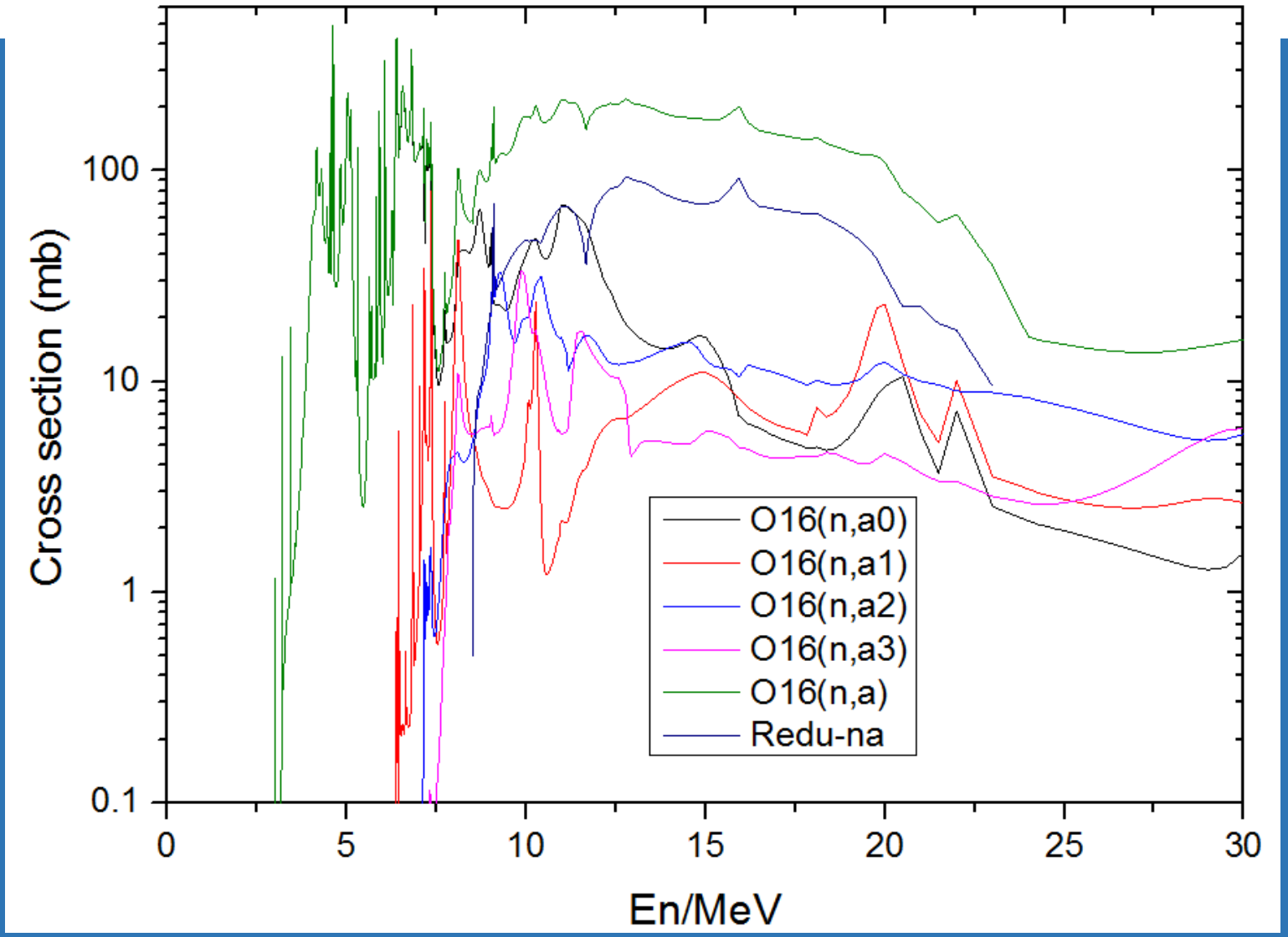

The contributions of discrete low energy levels and continuous high energy levels in (n, a).

5 Integral cross section calculation values

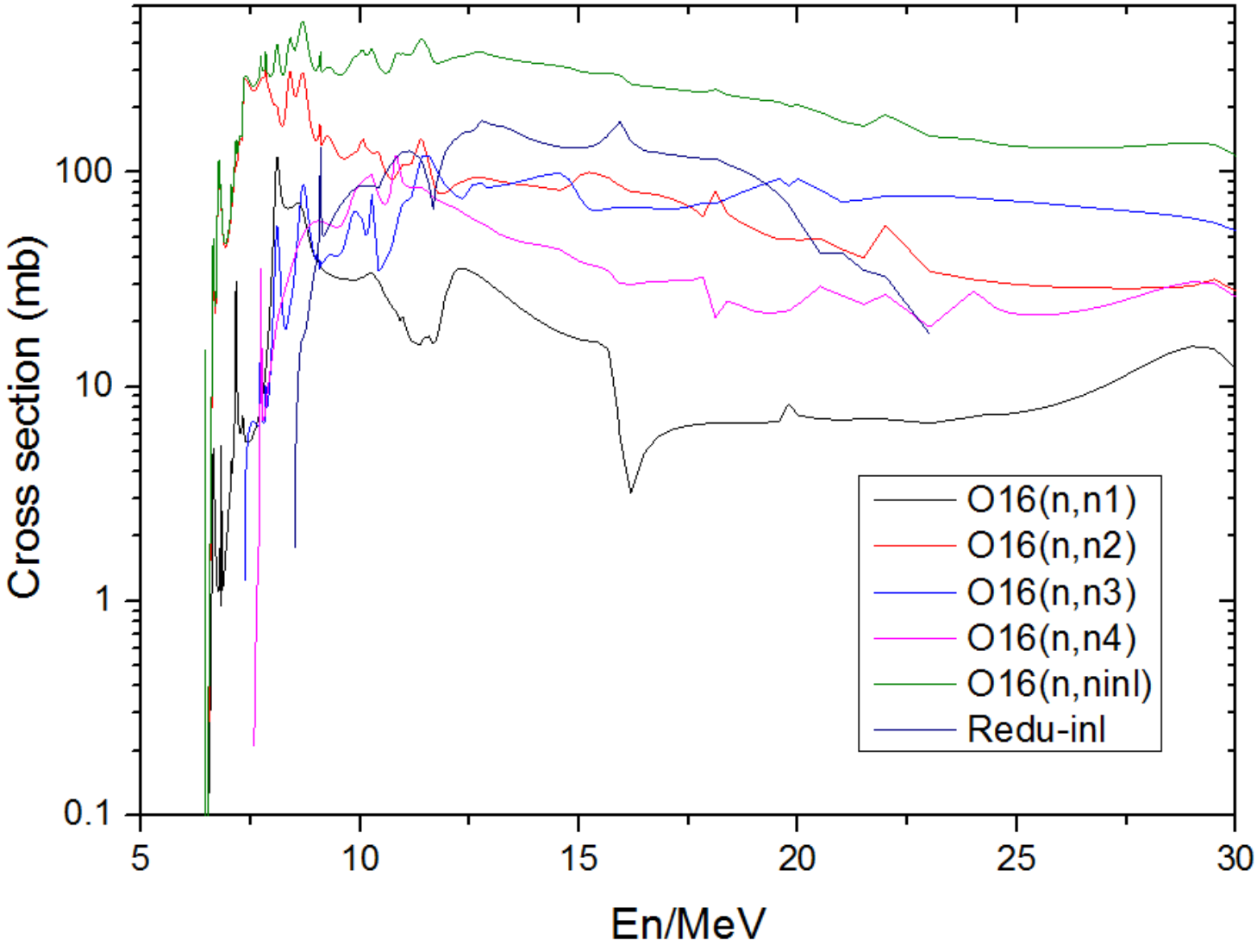

The contributions of discrete low energy levels and continuous high energy levels in (n, inl).

5 Integral cross section calculation values

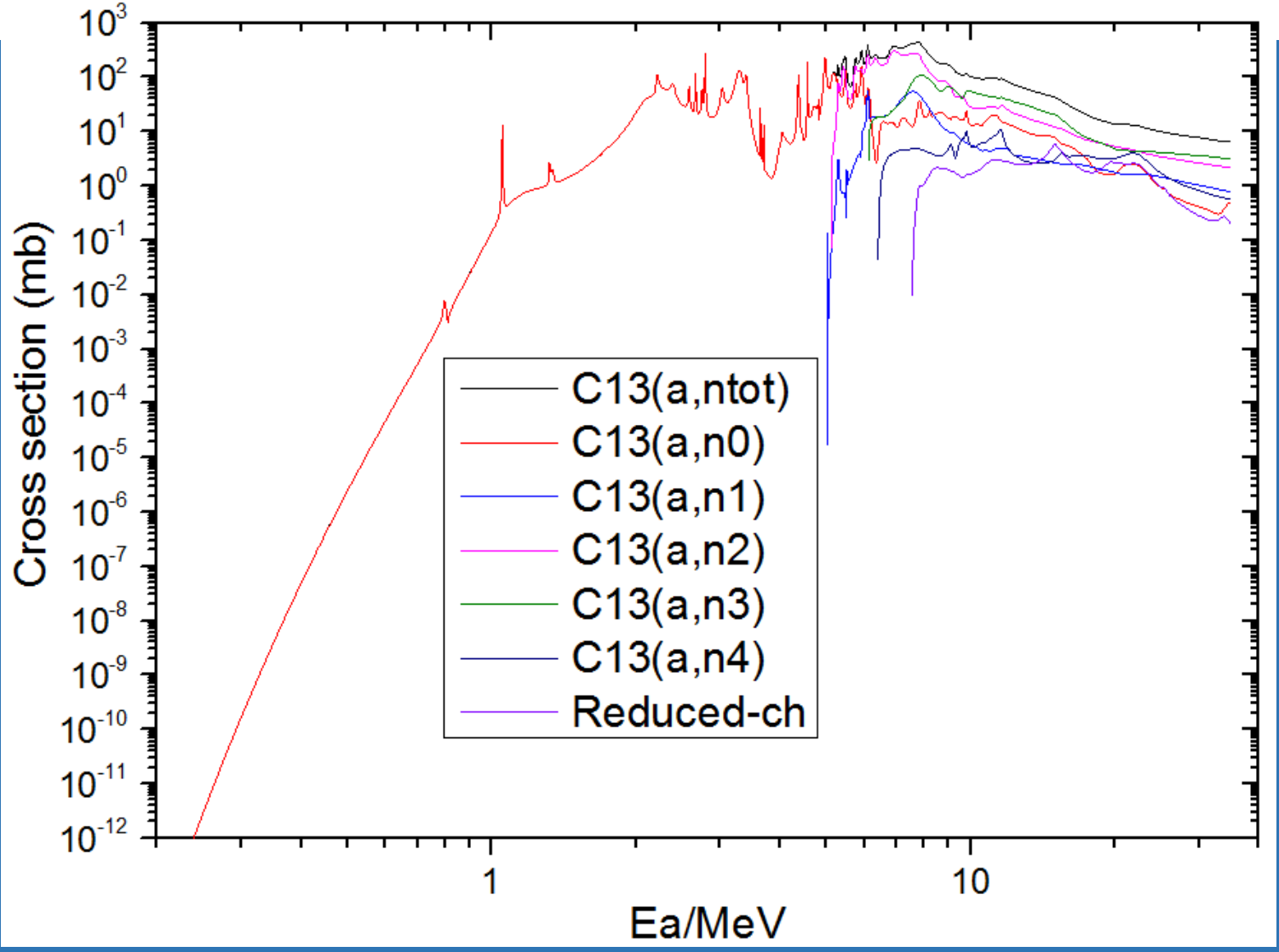

The (α, ntot), (α, n0), (α, n1), (α, n2), (α, n3), (α, n4). The (α, n2) is much bigger than(α, n1).

5 Integral cross section calculation values

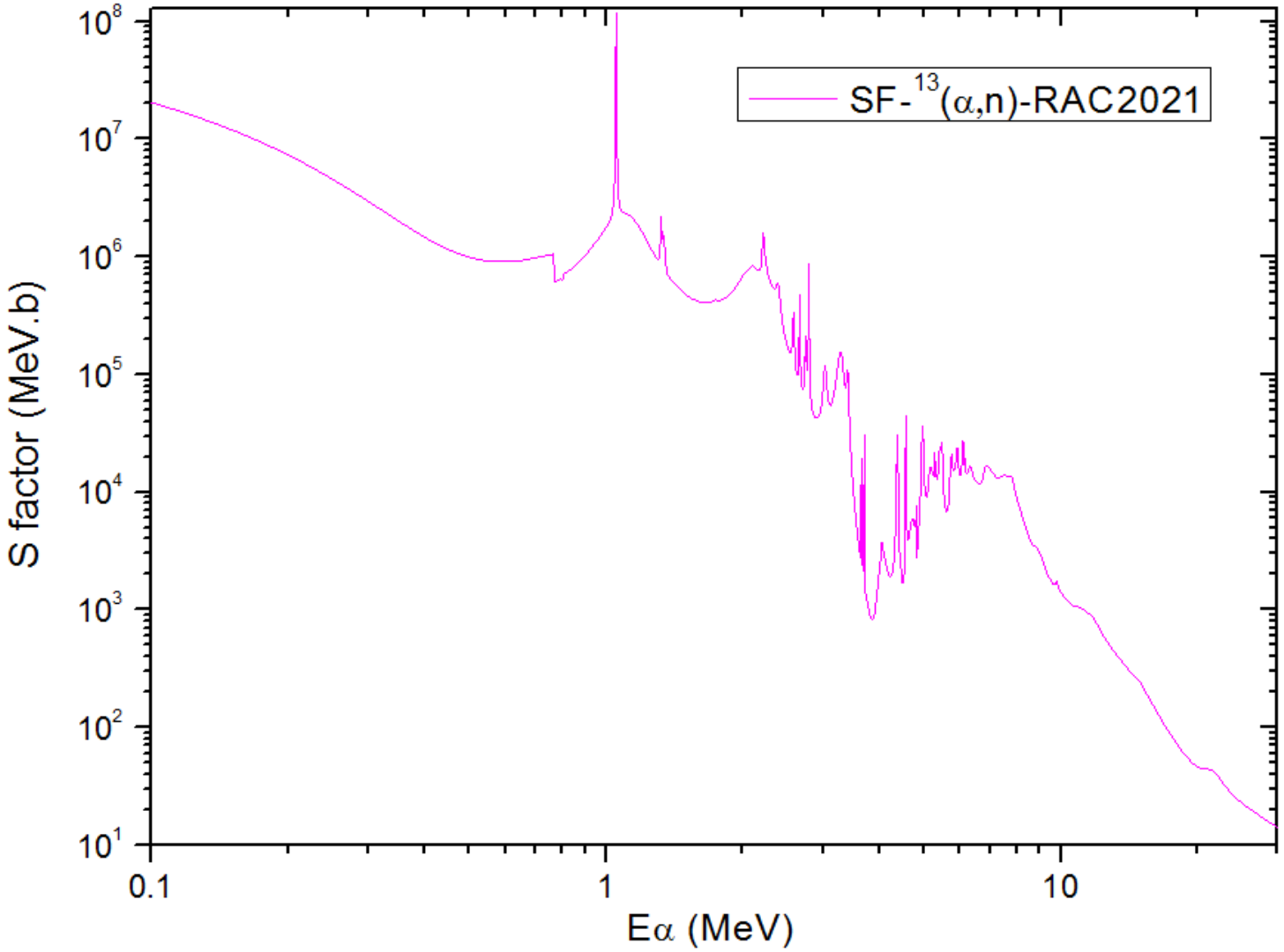

The S factor of (α, ntot), it need improved near 0.8 MeV, which is the junction of two groups of data, and all experimental data have not been normalized.

5 Integral cross section calculation values

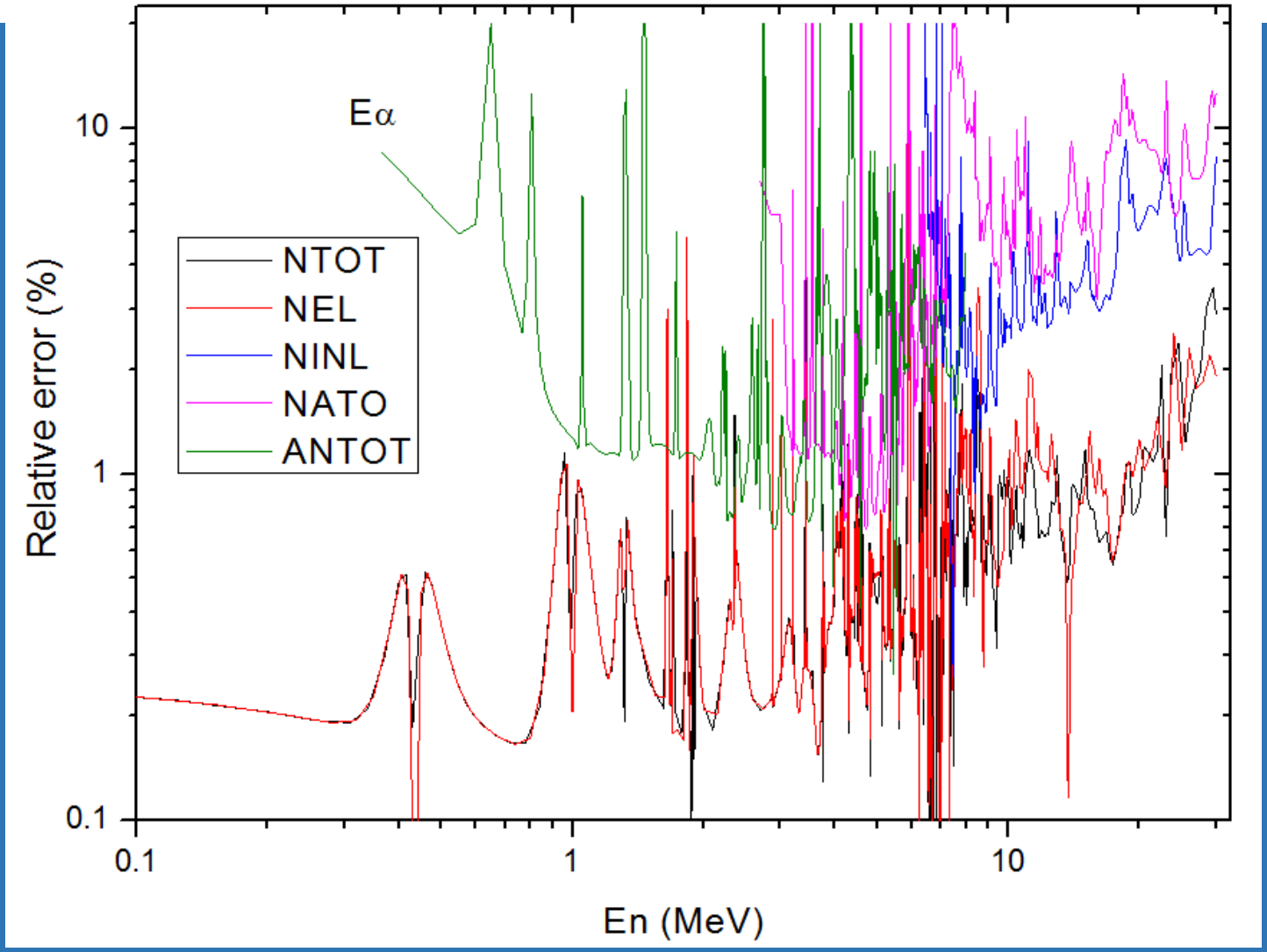

The relative error of evaluation values of (n, tot), (n, el), (n, inl), (n,α) and (α, n).

5 Integral cross section calculation values

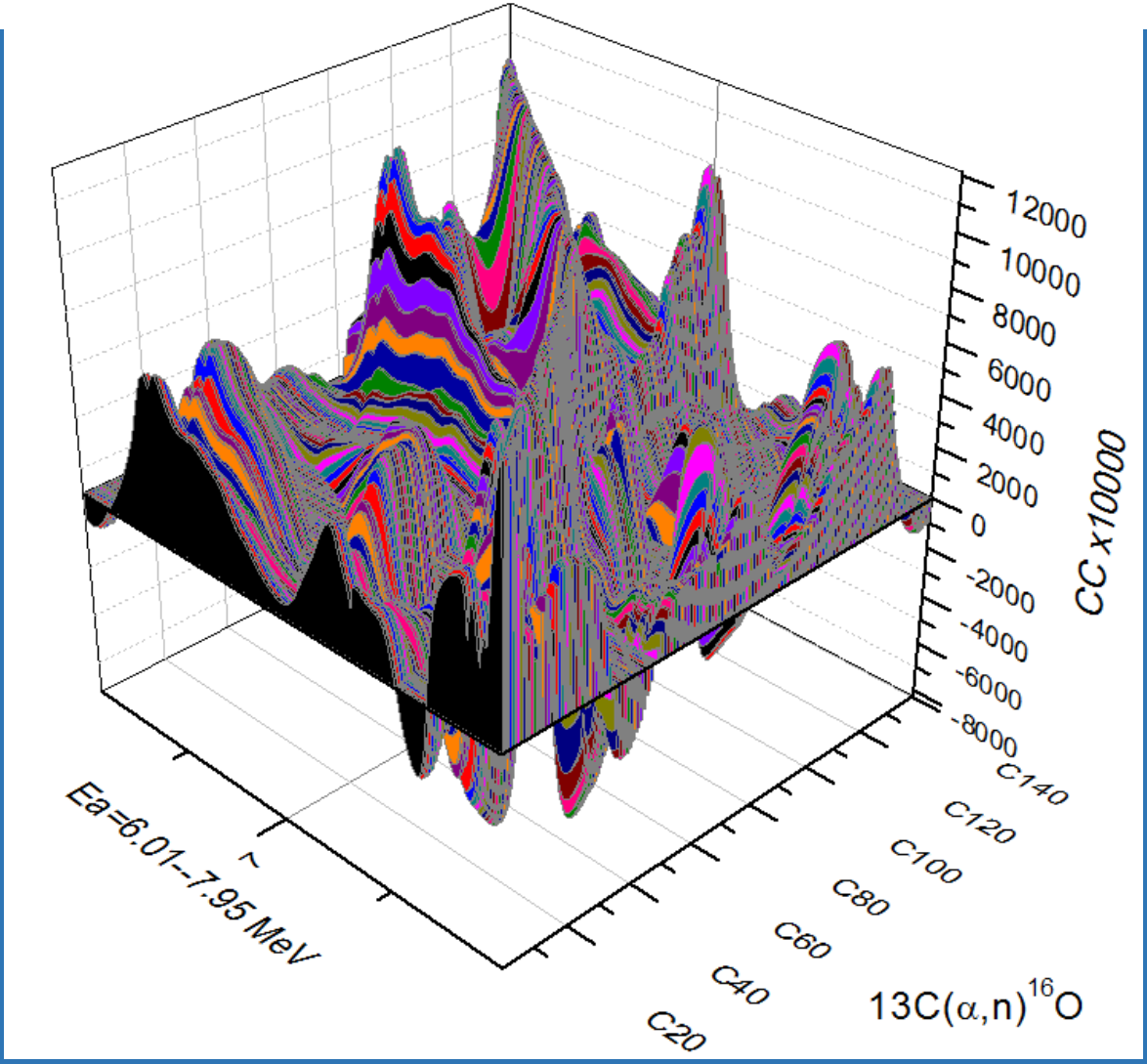

The correlation coefficient of (α, n) for E_α=6.01 to 7.95 MeV.

contents

6 An evaluation file with ENDF-6 Formats.

The following documents are available on a data basis.

MT=1 TOTAL CROSS SECTION
MT=2 ELASTIC SCATTERING CROSS SECTION
MT=4 INELASTIC CROSS SECTION
MT=51 Ex= 6.0494 MeV
MT=52 Ex= 6.129893 MeV
MT=53 Ex= 6.9171 MeV
MT=54 Ex= 7.11685 MeV
MT=91 Ex= 8.8719 MeV,(N,N'CONTINUUM) CROSS SECTION
MT=16 (N,2N) CROSS SECTION
MT=22 (N,NALPHA) CROSS SECTION
MT=23 (N,N3ALPHA) CROSS SECTION
MT=28 (N,NP) CROSS SECTION
MT=32 (N,ND) CROSS SECTION
MT=41 (N,2NP) CROSS SECTION (Reduced)
MT=44 (N,N2P) CROSS SECTION (Reduced)
MT=45 (N,NPALPHA) CROSS SECTION (Reduced)

6 An evaluation file with ENDF-6 Formats.

They do not have definitive experimental data, so there is a great deal of uncertainty in the final classification of contributions.

MT=102 (N,GAMMA) CROSS SECTION
MT=103 (N,P) CROSS SECTION
MT=104 (N,D) CROSS SECTION
MT=105 (N,T) CROSS SECTION
MT=107 (N,ALPHA) CROSS SECTION
MT=108 (N,2ALPHA) CROSS SECTION
MT=800 (N,ALPHA0) CROSS SECTION TO 13C GROUND STATE
MT=801-803 (N,ALPHA) CROSS SECTION TO EXCITED LEVELS OF 13C

MF=4 ANGULAR DISTRIBUTIONS
MT=2 ELASTIC NEUTRON ANGULAR DISTRIBUTIONS
MT=51-54 DISCRETE (N,N') ANGULAR DISTRIBUTIONS
MT=800 DISCRETE(N,ALPHA0) ANGULAR DISTRIBUTIONS

MF=33
MF=34

The covariance matrix is so large that it is not sure which reaction channels need to be provided with the covariance matrix.

contents

7 Discussion

1. The evaluation method has been introduced in detail in NDC(NDS)-0791.pdf and not be repeated here. The main feature of RAC is to adopt the χ^2 expression of 'General Least-Squares'(GLS), instead of 'Approximate Least-Squares' (ALS) which being widely used by now. When GLS was used to fit experimental data at the beginning, χ^2 was relatively large and PPP was easy to occur, which was caused by too large systematic error. In the process of RAC evaluation, the χ^2 of GLS and the χ^2 of ALS are displayed at the same time. By carefully adjusting the normalization coefficient and reducing the systematic error as much as possible, the χ^2 (GLS) and χ^2 (ALS) are closer and closer, until they are satisfied. In other words, adopting GLS will force the evaluator to carefully normalize the experimental data, so that the experimental data set can achieve a high degree of internal consistency, so as to obtain the most reliable evaluation value and corresponding covariance matrix.

7 Discussion

2. Due to theoretical limitations, the contribution of 'multibody channel ' must be expressed as' total width of reduced channel '; Due to the limitation of PC computing power, the contribution of 'high discrete energy levels' also needs to be expressed in terms of ' reduced channel total width '. They often do not have definitive experimental data, so there is rather large uncertainty in the final classification of contributions.

3. The covariance matrix is so large that it is not sure which reaction channels need to be provided with the covariance matrix.

4. So far, we have systematically analyzed all light nuclei (A = 1 to 16) systems, and preliminary results have been obtained. The next step is to study how to obtain a 'double differential cross section', such as that of ^{9}Be (n, 2n), based on RAC analysis.

Appendix I. Elastic scattering cross section of 16O(n, n)16O

Much more NNDA were used, here show a part of them (100+).

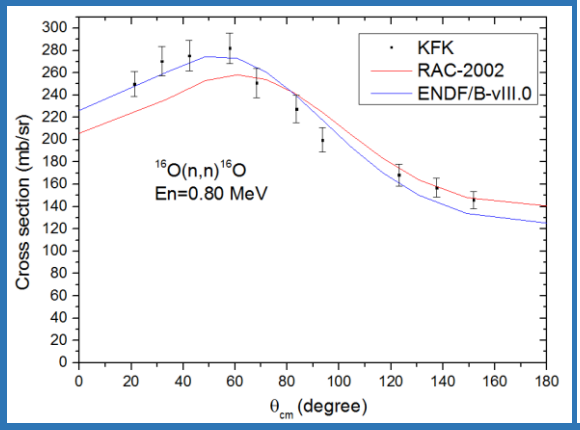

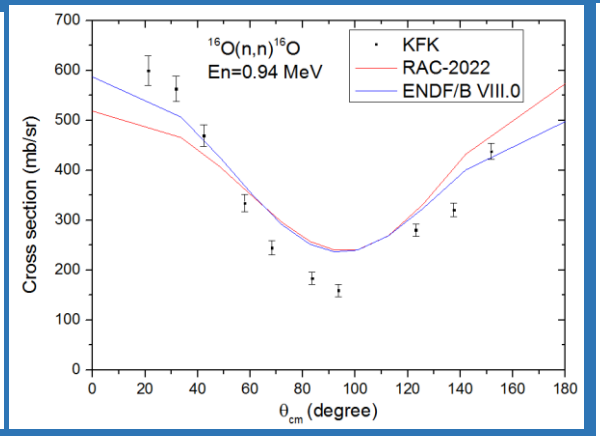

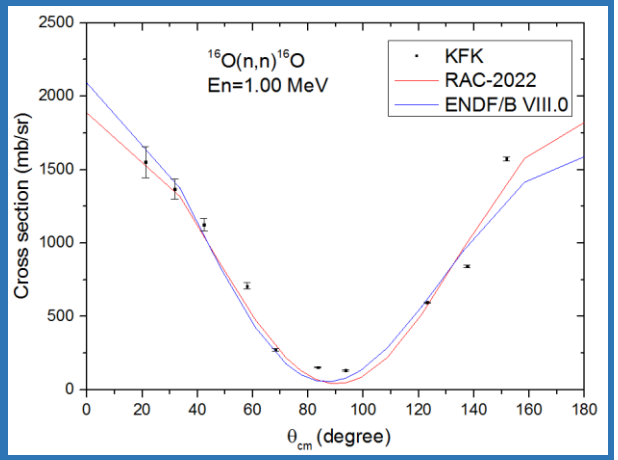

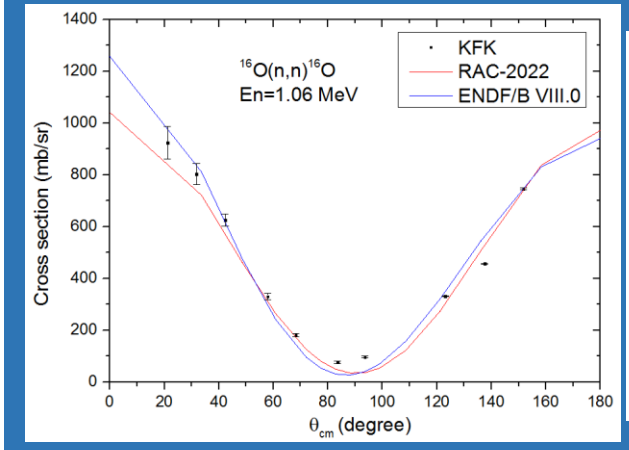

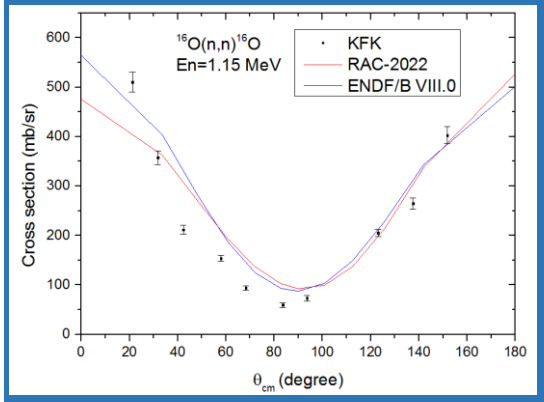

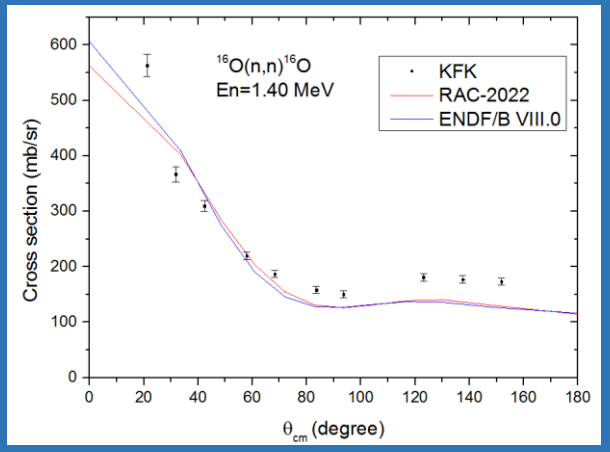

Thanks for your attention!!